

RUB-TPII-62/93
January 1994

Fermion Sea Along the Sphaleron Barrier

Dmitri Diakonov^{*1}, Maxim Polyakov^{*},
Peter Sieber[◊], Jörg Schaldach[◊] and Klaus Goeke[◊]

**St. Petersburg Nuclear Physics Institute, Gatchina, St.Petersburg 188350, Russia*

◊Inst. für Theor. Physik II, Ruhr-Universität Bochum, D-44780 Bochum, Germany

Abstract

We study the fermion Dirac sea along the minimal energy path between topologically distinct vacua in the electroweak theory. We follow in detail the interplay between the bound state and the continuum in the fermion creation/annihilation, as one passes from one vacuum to another. We calculate the quantum correction to the classical energy of the sphaleron barrier, arising from the fermion sea, and its contribution to the baryon number violation rate for non-zero temperatures. We find that the fermion fluctuations suppress that rate if the mass of the top quark is large enough.

¹Alexander von Humboldt Forschungspreisträger

e-mail:

diakonov@lnpi.spb.su

maxpol@lnpi.spb.su

peters@proton.tp2.ruhr-uni-bochum.de

joergs@proton.tp2.ruhr-uni-bochum.de

goeke@hadron.tp2.ruhr-uni-bochum.de

1 Introduction

The fact that the potential energy of the Yang–Mills fields is periodic in a certain topological functional of the gauge fields, called the Chern–Simons number N_{CS} , was shown quite a long time ago by Faddeev [1] and Jackiw and Rebbi [2]. In an unbroken Yang–Mills theory (like QCD) the classical energy barrier between the topologically distinct vacua can be made infinitely small due to the scale invariance. In a spontaneously broken theory (like the electroweak one) the scale invariance is explicitly violated by the Higgs v.e.v., and the height of the barrier is of the order of m_W/α , where m_W is the W -boson mass and $\alpha = g^2/4\pi$ is the $SU(2)$ gauge coupling.

Transitions from one vacuum to a topologically distinct one over this barrier cause a change in the baryon and lepton number by one unit per fermion doublet due to the axial anomaly [3]. Hence, this transition is a baryon and lepton number violating process and therefore of great physical significance. Although it is suppressed under ordinary conditions [3], its rate can become large at high densities [4, 5], high temperatures [6] or high particle energies [7, 8]. Thus, it could have occurred in the early universe [9, 10], and an exact determination of the transition rate is important to understand the excess of matter over antimatter.

The static configuration of the Yang–Mills (YM) and Higgs (H) field corresponding to the top of the barrier and having $N_{CS} = 1/2$, called sphaleron, was first found by Dashen, Hasslacher and Neveu [11] and, in the context of the electroweak theory, rediscovered by Klinkhammer and Manton [12]; its energy depends somewhat on the H -to- W mass ratio. Moreover, a continuous set of static configurations of W - and H -fields, leading from a vacuum at $N_{CS} = 0$ to another at $N_{CS} = 1$ and passing through the sphaleron at $N_{CS} = 1/2$, was presented by Akiba, Kikuchi and Yanagida (AKY) [13] (see also ref. [14]) who minimized the Yang–Mills and Higgs potential energy for a given value of N_{CS} . This set of configurations describes a pass in the potential energy surface over the Hilbert space of fields, the sphaleron corresponding exactly to the saddle point of the pass. As most of the workers in the field, we shall simplify the actual electroweak theory by neglecting the Weinberg angle, i.e. reducing it to the pure $SU(2)$ case (without the $U(1)$) and considering the simplest case of one Higgs doublet. It should be mentioned that the sphaleron barrier has also been found for non-zero Weinberg angle [15]; however the difference to the

idealized case does not seem to be significant.

The purpose of this paper is to study fermion field fluctuations around the whole sequence of static YM–H configurations leading from $N_{CS} = 0$ to 1. To this end we investigate the behaviour of the Dirac sea of fermions as one passes the sphaleron barrier. This is of great methodological interest, since, as mentioned above, the baryon and lepton numbers are changed during this passage owing to the axial anomaly. We follow in detail this phenomenon. The discrete level has previously been studied in [16]. The complete Dirac spectrum, however, is calculated for the first time in this work. We apply these results to determine the fermionic contribution to the energy of the configurations on the path from $N_{CS} = 0$ to $N_{CS} = 1$. This contribution is suppressed by the factor $\alpha = g^2/4\pi \approx 0.04$ relative to the classical one, but it also contains the large factor N_f which is 12 for the real world. It is reasonable to consider the range of parameters $\alpha \ll \alpha N_f \ll 1$ where the fermionic energy is a first order correction to the classical energy, but might have a considerable numerical value. In the case $\alpha N_f \sim 1$ one would have to solve self-consistent equations for a sphaleron coupled to fermions.

Having calculated the Dirac spectrum we evaluate the temperature dependent corrections of the baryon number violation rate due to the fermionic fluctuations. For a realistic set of parameters $g = 0.67$, $N_f = 12$ ($2N_c + 3 = 9$ massless and $N_c = 3$ massive doublets), $m_H = m_W$, and m_t between $1.5 m_W$ and $2.5 m_W$ we find numerically that the fermionic contribution to the exponent of the Boltzmann factor increases the classical exponent by up to 65% in the temperature range $0.3 m_W \leq T \leq 1.5 m_W$, which can considerably suppress the baryon number changing sphaleron transition rate. The suppression increases dramatically with the top quark mass; at $m_t \approx 3 m_W$ the fermionic contribution to the exponent becomes as large as the classical one.

Finally our aim is to compute the baryon number and -density. We confirm the law $B = N_{CS}$ and show that for $N_{CS} \rightarrow 1$ the created baryon becomes a free, delocalized particle.

The paper is organized as follows: After recalling briefly the AKY [13] configurations along the barrier, we introduce the Dirac operator in the background field of those configurations and diagonalize it in a spherical basis. We show how the fermionic energy contributions can be extracted from the Dirac spectrum. The energy of the Dirac sea is known to be divergent. Using a proper time regularization scheme, we separate the divergencies and combine them

with the classical energy whose parameters become renormalized. We next consider the high temperature transition rate and derive the fermionic part of its prefactor. The temperature range in which the result can be applied will be discussed. Finally we present our numerical results and discuss them in the last section of the paper.

The simplified version of the standard electroweak theory that we are going to study describes the $SU(2)$ YM field interacting with the H doublet, and one left-handed fermion doublet showing a Yukawa coupling to two right-handed singlets. In principle, an $SU(2)$ theory with an odd number of left-handed fermion doublets is not properly defined because of the so-called global $SU(2)$ anomaly [17]. However, as we shall see in practical terms we do not encounter any problems related to that anomaly in the present work.

The Lagrangian is thus:

$$\begin{aligned}\mathcal{L} &= \mathcal{L}_{YMH} + \mathcal{L}_F, \\ \mathcal{L}_{YMH} &= -\frac{1}{4g^2}F_{\mu\nu}^a F^{a\mu\nu} + (D_\mu\Phi)^\dagger(D^\mu\Phi) - \frac{\lambda^2}{2}\left(\Phi^\dagger\Phi - \frac{v^2}{2}\right)^2, \quad (1.1)\end{aligned}$$

$$\mathcal{L}_F = \bar{\psi}_L i\gamma^\mu D_\mu \psi_L + \bar{\chi}_R i\gamma^\mu \partial_\mu \chi_R - \bar{\psi}_L M \chi_R - \bar{\chi}_R M^\dagger \psi_L \quad (1.2)$$

with $F_{\mu\nu}^a = \partial_\mu A_\nu^a - \partial_\nu A_\mu^a + \varepsilon^{abc} A_\mu^b A_\nu^c$ and the covariant derivative being defined as $D_\mu = \partial_\mu - iA_\mu^a \tau^a/2$. M is a 2×2 matrix composed of the Higgs field components $\Phi = \begin{pmatrix} \phi^+ \\ \phi^0 \end{pmatrix}$, and the Yukawa couplings h_u, h_d :

$$M = \begin{pmatrix} h_u \phi^{0*} & h_d \phi^+ \\ -h_u \phi^{+*} & h_d \phi^0 \end{pmatrix}. \quad (1.3)$$

ψ_L means the $SU(2)$ fermion doublet $\begin{pmatrix} u_L \\ d_L \end{pmatrix}$, and with χ_R we denote the pair of the singlets u_R, d_R .

2 AKY Configurations

In order to minimize the energy of the static YM–H fields at a given value of the Chern–Simons number,

$$N_{CS} = \frac{1}{16\pi^2} \int d^3\mathbf{r} \varepsilon_{ijk} \left(A_i^a \partial_j A_k^a + \frac{1}{3} \varepsilon^{abc} A_i^a A_j^b A_k^c \right), \quad (2.1)$$

one has to minimize the quantity

$$\mathcal{E} = E_{class} + 2\xi N_{CS}. \quad (2.2)$$

Here ξ is a Lagrange multiplier and E_{class} is the energy of the static YM–H configuration which, in accordance with eq. (1.1), is

$$E_{class} = \int d^3\mathbf{r} \left\{ \frac{1}{2g^2} (B_i^a)^2 + (D_i\Phi)^\dagger (D_i\Phi) + \frac{\lambda^2}{2} \left(\Phi^\dagger \Phi - \frac{v^2}{2} \right)^2 \right\}, \quad (2.3)$$

where we have written $B_i^a = \frac{1}{2}\varepsilon_{ijk}F_{jk}^a$.

At the classical level the H field develops the v.e.v. $\langle\phi^0\rangle = v/\sqrt{2}$, $\langle\phi^+\rangle = 0$, and the W boson field A_μ^a gets a mass $m_W = gv/2$, while the H field mass is $m_H = \lambda v$. We choose the commonly used temporal gauge $A_0^a(x) \equiv 0$ and look for the minimum of eq. (2.2) in a spherically-symmetric "hedgehog" form [11, 12, 13]:

$$\begin{aligned} A_i^a(\mathbf{r}) &= \varepsilon_{aij}n_j \frac{1 - A(r)}{r} + (\delta_{ai} - n_a n_i) \frac{B(r)}{r} + n_a n_i \frac{C(r)}{r}, \\ \Phi(\mathbf{r}) &= \frac{v}{\sqrt{2}} [H(r) + i(\mathbf{n}\phi)G(r)] \begin{pmatrix} 0 \\ 1 \end{pmatrix}, \end{aligned} \quad (2.4)$$

where $r = |\mathbf{r}|$ and $\mathbf{n} = \mathbf{r}/r$.

Gauge transformation which do not change the above ansatz are given by

$$\Phi \rightarrow U\Phi, \quad A_i \rightarrow U A_i U^\dagger + iU\partial_i U^\dagger, \quad U = \exp[i(\mathbf{n}\phi)P(r)], \quad (2.5)$$

with $A_i \equiv A_i^a \tau^a/2$. Indeed, under this gauge transformation the functions A, B, C, H, G transform as follows:

$$\begin{aligned} A(r) &\rightarrow A(r) \cos 2P(r) - B(r) \sin 2P(r), \\ B(r) &\rightarrow B(r) \cos 2P(r) + A(r) \sin 2P(r), \\ C(r) &\rightarrow C(r) + 2rP'(r), \\ H(r) &\rightarrow H(r) \cos P(r) - G(r) \sin P(r), \\ G(r) &\rightarrow G(r) \cos P(r) + H(r) \sin P(r). \end{aligned} \quad (2.6)$$

This gauge freedom can be used to simplify the minimization of the functional (2.2) for which we choose a gauge with $C(r) \equiv 0$. This fixes the gauge transformation (2.5) up to a global rotation with a constant P .

We next introduce dimensionless quantities,

$$x = r \frac{gv}{2} = rm_W, \quad \kappa^2 = \frac{4\lambda^2}{g^2} = \frac{m_H^2}{m_W^2}, \quad \zeta = \frac{\alpha\xi}{2\pi m_W}, \quad (2.7)$$

and will measure the energy in units of $M_0 = 2\pi m_W/\alpha$. The functional (2.2) becomes:

$$\begin{aligned} \frac{\mathcal{E}}{M_0} = & \frac{1}{2\pi} \int_0^\infty dx \left[A'^2 + B'^2 + \frac{(A^2 + B^2 - 1)^2}{2x^2} + 2x^2(G'^2 + H'^2) - 4BGH \right. \\ & \left. + 2A(G^2 - H^2) + (1 + A^2 + B^2)(G^2 + H^2) + \frac{\kappa^2}{2}x^2(G^2 + H^2 - 1)^2 \right] \\ & + 2\zeta N_{CS}. \end{aligned} \quad (2.8)$$

The Chern–Simons number N_{CS} given by eq. (2.1) is only well defined for boson fields which are continuous and vanish fast enough at infinity. In terms of the hedgehog ansatz (2.4) this means we have to use a gauge with $A(0) = A(\infty) = 1$, $B(0) = B(\infty) = 0$ and $C(0) = C(\infty) = 0$, which is not fulfilled for fields with $C(r) \equiv 0$ which minimize the functional (2.8). Hence, before inserting ansatz (2.4) into eq. (2.1) we have to gauge rotate the fields. A suitable transformation is obtained from eq. (2.6) with $P(0) = -\varphi(0)/2$, $P(\infty) = -\varphi(\infty)/2$ where $\varphi(r) = \arg[A(r) + iB(r)]$. By substitution of the gauge rotated fields into eq. (2.1) we obtain in terms of the *unrotated* fields with vanishing C :

$$N_{CS} = \frac{1}{2\pi} \int_0^\infty dx (A'B - B'A) + \frac{1}{2\pi} (\varphi(\infty) - \varphi(0)). \quad (2.9)$$

Note that N_{CS} does not depend on the detailed shape of $P(r)$. It is therefore possible to perform the minimization of \mathcal{E} with the unrotated fields A and B by inserting (2.9) into eq. (2.8). Afterwards, the solution can easily be transformed into any other gauge by (2.6).

In order to find the minimum of \mathcal{E} one has to solve the Euler–Lagrange eqs. for A, B, G, H with boundary conditions compatible with the finiteness of \mathcal{E} . The details are given in app. A. One finds a family of solutions labelled by ζ ; $-1 < \zeta < 1$. From eq. (2.9) one then gets the relation between N_{CS} and ζ which should be used to express E_{class} through N_{CS} . The values of $\zeta = -1, 0$ and 1 correspond to $N_{CS} = 0, 1/2$ and 1 , respectively.

If one is interested in the case of finite fermion number density, one has to add a term $2\mu N_{CS}$ to the energy functional (2.3), where μ is the chemical potential for fermions [4, 5]. Since the form of the functional to be minimized is exactly the same as in the Lagrange multiplier approach, used to find the minimal energy barrier between the topologically distinct vacua, one proceeds in the same way as above. The only difference is that in the case of $\mu \neq 0$ the energy is $E_{class}(\mu) = E_{class}(0) + 2\mu N_{CS}$. We present the minimal energy curves

as a function of the Chern–Simons number for different values of the chemical potential μ in Fig. 1. At $\mu = 0$ we reproduce the curve of ref. [13]. It can be seen that at $\mu = \mu_{crit} = 2\pi m_W/\alpha$ the energy barrier disappears – a fact which was anticipated previously from analyzing vacuum stability in the presence of finite baryon density [4, 5]. At $\mu < \mu_{crit}$ the decay of a state with finite baryon density is given by tunneling “bounce” trajectories, found for small μ in ref. [5]. It is a challenge for future work to determine the decay rate of a high-density state for any μ .

One should not be irritated by the cusps of the curve at integer N_{CS} : the “coordinate” N_{CS} is a quadratic functional of the gauge field, and in a more natural coordinate the curve should be quadratic in the minima. To illustrate this, we have considered a 2-dimensional σ model with a mass term, which mimics the 4-d electroweak theory. In this model the minimal-energy configurations can be found analytically (D.Diakonov, V.Petrov and M.Polyakov, unpublished), and the energy barrier is described by the simple but exact formula $E = const |\sin \pi N_{CS}|$, also exhibiting cusps at integer N_{CS} . However, if one sticks to just one degree of freedom (N_{CS}), one should ask what is the kinetic energy along this particular “coordinate”. In the 2-d model this question can be answered exactly, and the restricted kinetic energy turns out to be $\dot{N}_{CS}^2 M(N_{CS})/2$ where the effective mass is $M(N_{CS}) = const / |\sin \pi N_{CS}|$, being singular at integer N_{CS} . Therefore, if one would replace N_{CS} by a coordinate X which would have a normal kinetic energy $\dot{X}^2/2$, the potential energy would behave normally at the minima – as X^2 .

3 Dirac Equation and Fermion Spectrum

We are now starting to investigate the Dirac continuum and the fermion discrete level in the background field of the static minimal-energy configurations described in the previous section.

We define the Dirac Hamiltonian as the operator \mathcal{H} appearing when one rewrites the Dirac equation following from eq. (1.2) in the form

$$\left(i \frac{\partial}{\partial t} - \mathcal{H} \right) \Psi = 0. \quad (3.1)$$

Using the representation

$$\gamma^0 = \begin{pmatrix} 1 & 0 \\ 0 & -1 \end{pmatrix}, \quad \gamma^i = \begin{pmatrix} 0 & \sigma_i \\ -\sigma_i & 0 \end{pmatrix}, \quad \gamma_5 = \begin{pmatrix} 0 & 1 \\ 1 & 0 \end{pmatrix}, \quad (3.2)$$

we can reduce the eight-spinors ψ_L, χ_R to four-spinors $\tilde{\psi}_L, \tilde{\chi}_R$ by the definition

$$\psi_L \equiv \frac{1}{\sqrt{2}} \begin{pmatrix} \tilde{\psi}_L \\ -\tilde{\psi}_L \end{pmatrix}, \quad \chi_R \equiv \frac{1}{\sqrt{2}} \begin{pmatrix} \tilde{\chi}_R \\ \tilde{\chi}_R \end{pmatrix}. \quad (3.3)$$

In the basis of the four-spinors $\tilde{\psi}_L, \tilde{\chi}_R$ the Hamiltonian \mathcal{H} is given by

$$\mathcal{H} = \begin{pmatrix} i\sigma_i D_i & M \\ M^\dagger & -i\sigma_i \partial_i \end{pmatrix}, \quad (3.4)$$

where M is defined in eq. (1.3). Here we have implied the $A_0 \equiv 0$ gauge.

For the sake of numerical simplicity in finding the eigenvalues of \mathcal{H} we would like to exploit fully the spherical symmetry of the AKY configurations. However, if the masses of the upper components of the isospin doublets are different from the lower ones, i.e. $h_u \neq h_d$, the spherical symmetry of the Dirac equation would be spoiled. For that reason we shall only consider the case of equal masses, $h_u = h_d = h$. This is certainly a very good approximation for all leptons and quarks whose masses are much less than m_W (which brings the scale into the problem) but it is not so good for the three (t, b) doublets. In Section 6 we will show how these massive doublets can be treated in the framework of this approximation.

In the hedgehog ansatz (2.4) the matrices M, M^\dagger have the form:

$$\begin{aligned} M &= m_F (H + i(\mathbf{n}\phi)G) \\ M^\dagger &= m_F (H - i(\mathbf{n}\phi)G) \end{aligned}, \quad m_F = \frac{hv}{\sqrt{2}}. \quad (3.5)$$

To find the fermion levels one has to solve the eigenvalue problem:

$$\mathcal{H} \begin{pmatrix} \tilde{\psi}_L \\ \tilde{\chi}_R \end{pmatrix} = E \begin{pmatrix} \tilde{\psi}_L \\ \tilde{\chi}_R \end{pmatrix}, \quad (3.6)$$

where

$$\mathcal{H} = \begin{pmatrix} i\sigma_i D_i & m_F (H + i(\mathbf{n}\phi)G) \\ m_F (H - i(\mathbf{n}\phi)G) & -i\sigma_i \partial_i \end{pmatrix}. \quad (3.7)$$

It is easy to check that the Dirac Hamiltonian \mathcal{H} (3.7) commutes with the so-called grand spin operator:

$$\hat{\mathbf{K}} = \hat{\mathbf{L}} + \hat{\mathbf{S}} + \hat{\mathbf{T}}, \quad (3.8)$$

where $\hat{\mathbf{L}}$ is the angular momentum, $\hat{\mathbf{S}}$ is the spin, and $\hat{\mathbf{T}}$ is the isospin operator:

$$\hat{L}^a = -i\epsilon^{abc}x_b\partial_c, \quad \hat{S}^a = \frac{1}{2}\sigma^a, \quad \hat{T}^a = \frac{1}{2}\tau^a, \quad (3.9)$$

with $\hat{\mathbf{S}}^2 = \hat{\mathbf{T}}^2 = 3/4$. Therefore, \mathcal{H} can be diagonalized in a basis of spherical harmonics with given grand spin K and its third component K_3 . According to the coupling rules of angular momenta, there are eight (in the case $K = 0$ only four) basis vectors for fixed values of K , K_3 and radial momentum p (Both signs of the energy are included). For the numerical diagonalization the basis is made finite by discretization of the radial momentum; the allowed values are denoted by p_n . For details the reader is referred to app. B. We call the matrix elements of \mathcal{H} in this basis $\mathcal{H}_{KK_3}^{rs}(p_m, p_n)$, where $r, s = 1 \dots 8$. Since they do not depend on K_3 we suppress this index in what follows; the degeneracy results in a factor $2K + 1$. The eigenvalues of $\mathcal{H}_K^{rs}(p_m, p_n)$ are denoted by ε_{Kn} or ε_λ , the ones of the free Dirac operator $\mathcal{H}^{(0)}$ are named $\varepsilon_{Kn}^{(0)}$ or $\varepsilon_\lambda^{(0)}$, given by $(\varepsilon_{Kn}^{(0)})^2 = p_n^2 + m_F^2$.

We have numerically calculated the eigenvalues ε_{Kn} as a function of N_{CS} for the transition from $N_{CS} = 0$ to $N_{CS} = 1$. The most interesting behaviour is found in the $K = 0$ sector, for which we plot some discretized eigenvalues in Fig. 2. At $N_{CS} = 0$ (vacuum), there are no discrete levels and the spectrum is symmetric; each level is two-fold degenerate. The levels of the lower continuum are occupied, the levels of the upper one are empty. When N_{CS} is increased, one level emerges from the lower continuum, travels all the way through the fermion mass gap, and finally reaches the upper continuum. This level stays occupied during the whole transition. As can be seen from Fig. 2., the other levels are slightly shifted upwards, each one replacing its predecessor. Eventually, at $N_{CS} = 1$ the spectrum looks exactly as at $N_{CS} = 0$, except that the first level of the upper continuum is now occupied, too. This shows that the transition between topologically distinct vacua is a baryon number violating process. Moreover, for intermediate (non-integer) values of N_{CS} we have confirmed numerically the law $B = N_{CS}$ following from the anomaly. Both the bound state level and the Dirac continuum contribute to the total baryon number B in this relation, and its proof requires an accurate gauge-invariant regularization of the Dirac sea, see Section 6. Previously, only the discrete level was investigated [16]; in this respect our results coincide with those of [16].

Our next aim is to calculate the total energy contribution E_{fer} of the fermions. This energy is simply given by the sum of the energies of all occupied states, relative to its value for the trivial vacuum at $N_{CS} = 0$. If we denote the energy of the discrete level which crosses zero by ε_{val} , we obtain

$$E_{fer} = \sum_{\varepsilon_\lambda^{(0)} < 0} (\varepsilon_\lambda - \varepsilon_\lambda^{(0)}) = \sum_{\varepsilon_\lambda < 0} \varepsilon_\lambda - \sum_{\varepsilon_\lambda^{(0)} < 0} \varepsilon_\lambda^{(0)} + \varepsilon_{val} \theta(\varepsilon_{val}) , \quad (3.10)$$

with the step function θ . Since $\text{Sp}(\mathcal{H} - \mathcal{H}^{(0)}) = 0$, we can also write

$$E_{fer} = -\frac{1}{2} \sum_{\lambda} \left(|\varepsilon_{\lambda}| - |\varepsilon_{\lambda}^{(0)}| \right) + \varepsilon_{val} \theta(\varepsilon_{val}) \equiv E_{sea} + \varepsilon_{val} \theta(\varepsilon_{val}) . \quad (3.11)$$

The sea energy E_{sea} can also be written as

$$E_{sea} = -\frac{1}{2} \left(\text{Sp} \sqrt{\mathcal{H}^2} - \text{Sp} \sqrt{\mathcal{H}^{(0)2}} \right) = -\frac{1}{2} \sum_K (2K+1) \sum_n \left(|\varepsilon_{Kn}| - |\varepsilon_{Kn}^{(0)}| \right) . \quad (3.12)$$

The quantity E_{fer} is in fact a fermion one-loop correction to the classical energy of the boson field, in particular it gives the quantum correction to the sphaleron mass (another quantum correction arises from boson field fluctuations around the sphaleron).

4 Renormalization

The aggregate energy of the Dirac sea (3.12) is divergent, since it is basically equivalent to the fermion loop in the external YM–H field. However, the electroweak theory is renormalizable which means that all divergencies can be absorbed by local counterterms to the Lagrangian. There are exactly four types of divergencies corresponding to four possible counterterms:

1. a divergency which can be absorbed in the B^2 counterterm, corresponding to the gauge coupling renormalization;
2. a divergency which can be absorbed in the $|D\Phi|^2$ counterterm, corresponding to the Higgs "wave function" renormalization;
3. a divergency which can be absorbed in the $\lambda^2|\Phi|^4$ counterterm, corresponding to the Higgs quartic coupling renormalization;
4. a divergency which can be absorbed in the $m_H^2|\Phi|^2$ counterterm, corresponding to the Higgs mass renormalization.

The last divergency is quadratic in contrast to the logarithmic divergencies in the first three cases.

Any renormalization assumes a certain "regularization scheme"; we shall use a cut-off in a proper time representation for the Dirac sea energy. This quantity can be written as

$$E_{sea} = -\frac{1}{2} \text{Sp} \sqrt{\mathcal{H}^2} = \frac{1}{4\sqrt{\pi}} \int_{\tau}^{\infty} \frac{dt}{t^{3/2}} \text{Sp} \exp(-t\mathcal{H}^2), \quad (4.1)$$

where Sp is a functional trace, \mathcal{H} is the Dirac Hamiltonian (3.7), and τ is the (inverse) ultra-violet cut-off, to be taken eventually to zero. A non-zero τ suppresses Dirac levels with high momenta, $|p| > 1/\sqrt{\tau}$. In eq. (4.1) and below we do not write the subtraction of the free Dirac sea explicitly, though we assume it.

Eq. (4.1) implies that the classical energy functional (2.3) contains bare couplings defined at the scale $1/\sqrt{\tau}$, such as the gauge coupling $g(1/\tau)$, the Higgs expectation value $v(1/\tau)$, etc. However, when one finds e.g. the classical mass of the sphaleron, one expresses it in terms of the physical couplings and Higgs expectation value, defined at the electroweak scale like m_W . Therefore, in order to use the standard values for the physical constants, a proper time integral between τ and $1/m_W^2$ has to be absorbed by the classical energy. To be more precise, we write:

$$\int_{\tau}^{\infty} \frac{dt}{t^{3/2}} \text{Sp} \exp(-t\mathcal{H}^2) = \int_{\tau}^{m_W^{-2}} + \int_{m_W^{-2}}^{\infty}. \quad (4.2)$$

In the first integral one can perform a semi-classical expansion as it deals with the spectral density of the operator \mathcal{H} at high momenta. The technique is explained e.g. in ref. [18]. We get for the divergent piece of the Dirac sea energy:

$$\begin{aligned} \frac{1}{4\sqrt{\pi}} \int_{\tau}^{m_W^{-2}} \frac{dt}{t^{3/2}} \text{Sp} \exp(-t\mathcal{H}^2) &= \frac{1}{16\pi^2} \int_{\tau}^{m_W^{-2}} dt \int d^3\mathbf{r} \left\{ -\frac{2g^2 m_F^2}{t^2 m_W^2} (\Phi^\dagger \Phi - \frac{v^2}{2}) \right. \\ &+ \frac{1}{t} \left[\frac{1}{6} (B_i^a)^2 + \frac{g^2 m_F^2}{m_W^2} |D_i \Phi|^2 + \frac{g^4 m_F^4}{2m_W^4} \left((\Phi^\dagger \Phi)^2 - \frac{v^4}{4} \right) \right] + \mathcal{O}(t^0) \left. \right\} \\ &\equiv \frac{1}{4\sqrt{\pi}} \int_{\tau}^{m_W^{-2}} \frac{dt}{t^{3/2}} [\text{Sp} \exp(-t\mathcal{H}^2)]_{\text{div}} + \text{finite terms}. \end{aligned} \quad (4.3)$$

We see that the quadratically ($1/t^2$) and logarithmically ($1/t$) divergent terms are exactly those entering the classical energy functional (2.3). Therefore, they can and should be combined with the bare constants of the corresponding terms in the classical energy – to produce renormalized physical constants at the scale of m_W . For example, the coefficients in front of the magnetic field energy, $B^2/2$, combine into

$$\frac{1}{g^2(1/\tau)} - \frac{1}{48\pi^2} \ln(m_W^2 \tau) = \frac{1}{g^2(m_W^2)}, \quad (4.4)$$

and similarly for the other three terms. (Eq. (4.4) is not the whole renormalization of the gauge constant since boson fluctuations also contribute to it).

Because the divergent part of (4.3) is combined with the classical energy, the renormalized Dirac sea energy is:

$$E_{sea}^{ren} = \frac{1}{4\sqrt{\pi}} \left(\int_{\tau}^{m_W^{-2}} \frac{dt}{t^{3/2}} \text{Sp exp}(-t\mathcal{H}^2) + \int_{m_W^{-2}}^{\infty} \frac{dt}{t^{3/2}} \text{Sp exp}(-t\mathcal{H}^2) - \int_{\tau}^{m_W^{-2}} \frac{dt}{t^{3/2}} [\text{Sp exp}(-t\mathcal{H}^2)]_{div} \right). \quad (4.5)$$

This expression is finite as $\tau \rightarrow 0$, and one can put $\tau = 0$ in it. Introducing a dimensionless variable $tm_W^2 \rightarrow t$ and measuring all quantities including the sea energy in units of m_W we get:

$$E_{sea}^{ren} = \frac{1}{4\sqrt{\pi}} \left(\int_0^{\infty} \frac{dt}{t^{3/2}} \text{Sp exp}(-t\mathcal{H}^2) - \int_0^1 \frac{dt}{t^{3/2}} [\text{Sp exp}(-t\mathcal{H}^2)]_{div} \right). \quad (4.6)$$

Though eq. (4.6) solves the problem of renormalization it is still not too practical from the numerical point of view. The divergence of the unrenormalized Dirac sea energy is due to the large contributions for high values of K . Therefore it is convenient to perform the renormalization subtraction for each K sector separately, like

$$E_{sea}^{ren} = \sum_K (2K+1)(E_K - E_K^{div}). \quad (4.7)$$

Then at each step one deals with perfectly finite quantities, and the summation in K is convergent.

To this end we calculate the divergent part (4.3) of the functional trace (i.e the quantity to be subtracted) in a basis of a complete set of eigenfunctions of the free Dirac Hamiltonian, given in app. B. From the definition of the trace we have:

$$\begin{aligned} \frac{1}{4\sqrt{\pi}} \int_0^1 \frac{dt}{t^{3/2}} \text{Sp exp}(-t\mathcal{H}^2) &= \sum_K (2K+1) \frac{1}{4\sqrt{\pi}} \int_0^1 \frac{dt}{t^{3/2}} \\ &\cdot \sum_{r=1}^8 \sum_{n=1}^{\infty} \int_0^R dx x^2 v_{K,i}^{(r)}(p_n, x) [\exp(-t\mathcal{H}_K^2)]_{ij} v_{K,j}^{(r)}(p_n, x). \end{aligned} \quad (4.8)$$

where \mathcal{H}_K is the Hamiltonian in the basis of the spherical eigenfunctions for given grand spin K and radial momentum p_n , in fact an 8×8 matrix, and $v_{K,i}^{(r)}(p_n, x)$ are the radial parts of the eigenfunctions. For details see app. B.

The semiclassical expansion in a given K sector corresponds to expanding the exponent in eq. (4.8) in powers of $\mathcal{H}_K - p_n$. The expansion is rather tedious and the result is lengthy. We present the final formula in app. D. There we also show that eq. (4.3) is reproduced from eq. (4.8) in the limit $R \rightarrow \infty$.

5 Renormalization at Non-Zero Temperatures²

Keeping in mind the application to the baryon number changing sphaleron transitions at non-zero temperatures (below the electroweak phase transition) we explain here how the renormalization is performed for the baryon number changing rate. This question has been addressed in [19] and [20] for the limit of high temperatures; it was demonstrated there how the theory is reduced to three dimensions. In our work we will not assume the high temperature limit but consider temperatures in the range (5.2) (see below). This leads to additional contributions which are not present in the limit of high temperature.

In principle we treat both fermion and boson fluctuations on equal footing. Our numerical calculations, however, are restricted to the corrections due to fermion fluctuations. The bosonic part will be numerically dealt with in a subsequent paper; so far it has been investigated in e.g. [20, 21, 22]. In an abelian $(1+1)$ dimensional model it is possible to calculate the sphaleron transition rate analytically. This has been done in [23] for boson loop corrections and in [24] for fermions.

The traditional starting point is the semi-classical Langer–Affleck formula [25, 26, 27] for the thermal transition rate Γ :

$$\Gamma = \frac{\beta \omega_-}{\pi} \operatorname{Im} F, \quad (5.1)$$

where ω_- is the negative boson eigenfrequency around the sphaleron, β is the inverse temperature and F is the free energy of the system.³ One can imagine introducing a small chemical potential for baryons so that the minima at integer N_{CS} become metastable, and $\operatorname{Im} F$ gets a precise meaning [6].

The Langer–Affleck formula works in the temperature range given approximately by [26]

$$\frac{\omega_-}{2\pi} \leq T \leq E_{class}^{ren}(T). \quad (5.2)$$

²This section was prepared in collaboration with V.Petrov and P.Pobylitsa.

³A question may arise about the applicability of this formula to the process under consideration since it implies that the transition occurs mainly *above* the sphaleron barrier. It is not too clear whether it is justifiable to treat such degrees of freedom as belonging to thermal equilibrium, and whether presumably perturbative field fluctuations above the barrier do actually lead to the baryon number change. Keeping in mind these reservations we nevertheless start from eq. (5.1).

If the temperature is lower than $\omega_-/2\pi$, the baryon number violation rate is dominated by transitions via periodic solutions of the classical Yang–Mills equations in Euclidean space [28]. In the case $T = 0$ these solutions reduce to instantons. Numerically the value of $\omega_-/2\pi$ was found to be $\approx 0.3 m_W$ for $m_H = m_W$ [20, 29]. The upper bound $E_{class}^{ren}(T)$ is the renormalized energy of the sphaleron barrier. As we show below, it depends on T ; it vanishes at some critical temperature T_c where the symmetry breaking of the electroweak theory disappears. Hence, eq. (5.2) implies $T \leq T_c$. We will discuss numerical results in Section 6, but let us mention here already that for $m_H = m_W$ and a reasonable value of the top quark mass, T_c is of the order m_W to $1.5 m_W$. We see thus that the domain of applicability of eq. (5.1) is rather restricted, and the reduction of the problem to three dimensions [20, 21, 22] implying $T \gg m_W$ does not seem to be justified in reality.

In the semi-classical approximation one takes the static sphaleron configuration as a saddle point for $\text{Im } F$, and has to compute the boson and fermion determinants around it. Special care must be taken towards the zero and negative modes of the boson small-oscillation operator; this problem has been solved in ref. [20, 21], and we denote the resulting factor by $\mathcal{N}_{0,-}$. The boson determinant below involves only positive eigenmodes, and is denoted by a prime. Eq. (5.1) can be written as

$$\Gamma = \frac{\omega_-}{2\pi} \mathcal{N}_{0,-} \left(\frac{\text{Det}_{bos}}{\text{Det}_{bos}^{(0)}} \right)'^{-\frac{1}{2}} \left(\frac{\text{Det}_{fer}}{\text{Det}_{fer}^{(0)}} \right) \exp(-\beta E_{class}^{bare}) , \quad (5.3)$$

where "bare" means that the classical mass of the sphaleron is computed with bare physical constants defined at some ultra-violet cut-off scale. The superscript (0) refers to the free (no field) determinants.

Let us denote by ω_n^2 the eigenvalues of the 3-dimensional quadratic form for boson fluctuations about the sphaleron and by ε_n the eigenvalues of the Dirac Hamiltonian for fermions; the same quantities with a superscript 0 stand for the corresponding no-field eigenvalues. Imposing boundary conditions periodic in time for bosons and antiperiodic for fermions, one immediately establishes the eigenvalues of the 4-dimensional small-oscillation operators ($k \in \mathbb{Z}$):

$$\lambda_{n,k}^{bos} = \omega_n^2 + \left(\frac{2k\pi}{\beta} \right)^2 , \quad \lambda_{n,k}^{fer} = \varepsilon_n + i \frac{(2k+1)\pi}{\beta} . \quad (5.4)$$

The determinants of eq. (5.3) are the products of these eigenvalues:

$$\begin{aligned} \left(\frac{\text{Det}_{bos}}{\text{Det}_{bos}^{(0)}} \right)'^{-\frac{1}{2}} &= \prod_n \prod_{k=-\infty}^{\infty} \frac{\lambda_{n,k}^{bos,0}}{\lambda_{n,k}^{bos}} = \prod_n \frac{\sinh(\omega_n^0 \beta/2)}{\sinh(\omega_n \beta/2)}, \\ \left(\frac{\text{Det}_{fer}}{\text{Det}_{fer}^{(0)}} \right) &= \prod_n \prod_{k=-\infty}^{\infty} \frac{\lambda_{n,k}^{fer}}{\lambda_{n,k}^{fer,0}} = \prod_n \frac{\cosh(\varepsilon_n \beta/2)}{\cosh(\varepsilon_n^0 \beta/2)}. \end{aligned} \quad (5.5)$$

At this point McLellan *et al.* [6, 20, 21] argue that in the case $T \gg m_W$, one should replace sinh by its argument and cosh by unity, since the 3-d eigenvalues ω_n, ε_n are of the order of m_W . We will show later that this replacement is justified, but as the condition $T \gg m_W$ is not compatible with the allowed range (5.2) we have to use the exact expressions in what follows. The determinants (5.5) can be identically rewritten as:

$$\prod_n \frac{\sinh(\omega_n^0 \beta/2)}{\sinh(\omega_n \beta/2)} = \exp \left\{ - \sum_n \frac{\beta}{2} (\omega_n - \omega_n^0) - \sum_n \ln \left[\frac{1 - e^{-\beta \omega_n}}{1 - e^{-\beta \omega_n^0}} \right] \right\}, \quad (5.6)$$

$$\prod_n \frac{\cosh(\varepsilon_n \beta/2)}{\cosh(\varepsilon_n^0 \beta/2)} = \exp \left\{ \sum_n \frac{\beta}{2} (|\varepsilon_n| - |\varepsilon_n^0|) + \sum_n \ln \left[\frac{1 + e^{-\beta |\varepsilon_n|}}{1 + e^{-\beta |\varepsilon_n^0|}} \right] \right\}. \quad (5.7)$$

The first terms in the exponents of eqs. (5.6, 5.7) make up the zero-point oscillation corrections to the bare sphaleron mass at zero temperatures:

$$E_{class}^{bare} + \sum_n \frac{1}{2} (\omega_n - \omega_n^0) - \frac{1}{2} \sum_n (|\varepsilon_n| - |\varepsilon_n^0|) \equiv E_1. \quad (5.8)$$

Both bosonic and fermionic sums are divergent but the divergencies are absorbed in the renormalization of the constants entering E_{class}^{bare} so that E_1 is finite. In Section 4 this renormalization was explicitly performed for the case of fermions.

The terms containing logarithms in eqs. (5.6, 5.7) depend on the temperature but are ultra-violet finite, since the large eigenvalues are cut by the Boltzmann factors. For a closer inspection of these terms we use spectral densities, in which the subtraction of the vacuum is included:

$$\sum_n \left[\ln(1 - e^{-\beta \omega_n}) - \ln(1 - e^{-\beta \omega_n^0}) \right] = \int_0^\infty dE \rho^{bos}(E) \ln \left(1 - e^{-\beta E} \right), \quad (5.9)$$

$$\sum_n \left[\ln(1 + e^{-\beta |\varepsilon_n|}) - \ln(1 + e^{-\beta |\varepsilon_n^0|}) \right] = \int_{-\infty}^\infty dE \rho^{fer}(E) \ln \left(1 + e^{-\beta |E|} \right). \quad (5.10)$$

We can derive a semiclassical high-energy expansion for the density, which is related to the expansion of eq. (4.3). If the latter one is written as

$$\text{Sp} \left(e^{-t\mathcal{H}^2} - e^{-t\mathcal{H}^{(0)2}} \right) = at^{-1/2} + bt^{1/2} + ct^{3/2} + \dots , \quad (5.11)$$

one finds:

$$\begin{aligned} \rho^{fer}(E) &= |E| \text{Sp} \left(\delta(\mathcal{H}^2 - E^2) - \delta(\mathcal{H}^{(0)2} - E^2) \right) \\ &= \frac{1}{\sqrt{\pi}} \left(a - \frac{b}{2} \frac{1}{E^2} + \frac{3c}{4} \frac{1}{E^4} + \dots \right) . \end{aligned} \quad (5.12)$$

We see that the first term corresponds to a constant spectral density ρ_∞^{fer} at large E (which, of course, is in perfect correspondence with the quadratic divergency of the Dirac energy). We get from eq. (4.3)

$$\rho_\infty^{fer} = \frac{a}{\sqrt{\pi}} = -\frac{g^2 m_F^2}{2\pi^2 m_W^2} \int d^3\mathbf{r} \left(\Phi^\dagger \Phi - \frac{v^2}{2} \right) \quad (5.13)$$

and a similar expression (but with a different coefficient) for ρ_∞^{bos} . Putting these ρ_∞ into eqs. (5.9, 5.10) we obtain for fermions:

$$\int_{-\infty}^{\infty} dE \rho_\infty^{fer} \ln \left(1 + e^{-\beta|E|} \right) = -\frac{g^2 m_F^2 T}{12 m_W^2} \int d^3\mathbf{r} \left(\Phi^\dagger \Phi - \frac{v^2}{2} \right) = \mathcal{O} \left(\frac{T m_F^2}{m_W^3} \right) . \quad (5.14)$$

This expression is obtained for each fermion doublet so that we have to sum over all doublets. Additionally, we must consider a similar result for bosons, where m_F^2 has to be replaced by $(3/4)(m_H^2 + 3m_W^2)$ in the prefactor [30]. At $T = \mathcal{O}(m_W/g)$ these terms can be of the same order as the (renormalized) classical zero-temperature energy of the sphaleron (divided by T), therefore in that range of temperatures one has to find a new sphaleron solution, with a new functional which includes the thermal part (5.14). Fortunately, it has the same form as already encountered in the classical energy functional (see eq. (2.3)); therefore, instead of solving anew the classical eqs. of motion one can use the non-thermal solution for the YM–H fields but with the parameter v replaced by the temperature dependent expression

$$v(T)^2 = v^2 - \frac{3m_H^2 + 9m_W^2 + 4 \sum_{\text{doubl.}} m_F^2}{6m_H^2} T^2 . \quad (5.15)$$

This leads to a temperature dependent renormalization of the masses:

$$\frac{m_H(T)}{m_H} = \frac{m_W(T)}{m_W} = \frac{m_F(T)}{m_F} = \frac{v(T)}{v} . \quad (5.16)$$

With this thermal renormalization of the parameters performed, one has to subtract the quantities $\rho_{\infty}^{bos, ferm}$ from $\rho^{bos, ferm}(E)$ in eqs. (5.9, 5.10). After the subtraction high E are suppressed as $1/E^2$ in the integrand so that in the limit $T \gg m_W$ the contributions from eqs. (5.9, 5.10) read:

$$\int_0^{\infty} dE \left(\rho^{bos}(E) - \rho_{\infty}^{bos} \right) \ln(\beta E), \quad (5.17)$$

$$\int_{-\infty}^{\infty} dE \left(\rho^{fer}(E) - \rho_{\infty}^{fer} \right) \ln 2. \quad (5.18)$$

Apart from the subtleties with the renormalization mentioned above, this is what one would naively get from eq. (5.5) by replacing the fermionic \cosh by unity and the bosonic \sinh by its argument, which corresponds to the recipe of [6, 20, 21]. However, we are not working in the high temperature limit but in the range eq. (5.2) so that we have to use the full formula for the sphaleron transition rate:

$$\Gamma = \frac{\omega_-}{2\pi} \mathcal{N}_{0,-} \exp\left(-\beta E_{tot}(T)\right), \quad (5.19)$$

where

$$E_{tot}(T) = E_{class}^{ren}(T) + E_{bos}^{temp} + E_{fer}^{temp}, \quad (5.20)$$

with

$$\begin{aligned} \beta E_{bos}^{temp} &= \beta \int_0^{\infty} dE \left(\rho^{bos}(E) - \rho_{\infty}^{bos} - \mathcal{O}(1/E^2) \right) \frac{E}{2} \\ &\quad + \int_0^{\infty} dE \left(\rho^{bos}(E) - \rho_{\infty}^{bos} \right) \ln \left(1 - e^{-\beta E} \right) \\ \beta E_{fer}^{temp} &= -\beta \int_{-\infty}^{\infty} dE \left(\rho^{fer}(E) - \rho_{\infty}^{fer} - \mathcal{O}(1/E^2) \right) \frac{|E|}{2} \\ &\quad - \int_{-\infty}^{\infty} dE \left(\rho^{fer}(E) - \rho_{\infty}^{fer} \right) \ln \left(1 + e^{-\beta |E|} \right). \end{aligned} \quad (5.21)$$

Here $E_{class}^{ren}(T)$ is the classical sphaleron mass with the temperature-renormalized values of the physical constants given by eqs. (5.15, 5.16). According to eqs. (5.20, 5.21) the classical mass gets corrections due to the temperature independent zero-point oscillations (the first terms of E_{bos}^{temp} and E_{fer}^{temp}) and due to temperature dependent terms (the last terms of E_{bos}^{temp} and E_{fer}^{temp}). The $\mathcal{O}(1/E^2)$ terms to be subtracted from the spectral densities correspond to the logarithmic divergencies written explicitly for the fermions in eq. (5.12).

The boson loop corrections βE_{bos}^{temp} are suppressed by the factor α so that they are usually discussed in context with the pre-exponential factor. Its investigation is not performed in this work. The fermionic contribution βE_{fer}^{temp}

is also suppressed by α , but it is enhanced by the number of fermionic species $N_f = 12$ so that its value can be considerable. We shall see in next section that it suppresses the transition rate significantly, especially for massive fermions.

6 Numerical Results and Discussion

In this section we present our numerical results. Since the dependence on the Higgs mass m_H turns out to be weak we decided to fix $m_H = m_W$ for all calculations presented in this section. We will briefly comment on the influence of m_H at the end of the section. All results are computed using the physical value $g = 0.67$ for the coupling constant.

Let us start by discussing the behaviour of the fermion spectrum and the contributions to the energy for the path from $N_{CS} = 0$ to $N_{CS} = 1$. The level crossing phenomenon has already been demonstrated in Fig. 2. Additionally, we have investigated the discrete level for various fermion masses m_F and our results agree with those of Kunz and Brihaye [16].

In the following we present numerical results for the fermionic energy E_{fer} , especially its sea part E_{sea}^{ren} , given by eqs. (3.10, 3.11) and eq. (4.6). Eq. (4.6) implies that the UV cut-off $\Lambda = 1/\sqrt{\tau}$ has to be taken to infinity. In practical terms, however, we always have to work with a finite Λ since our numerical basis must be finite. Therefore we calculate E_{sea}^{ren} as a function of Λ and extrapolate to its value $E_{sea}^{ren}(\infty)$ at $\Lambda = \infty$. From the semiclassical expansion of E_{sea} for high Λ we obtain the following dependence:

$$E_{sea}^{ren}(\Lambda) = E_{sea}^{ren}(\infty) - \frac{C}{\Lambda^2} + \mathcal{O}\left(\frac{1}{\Lambda^4}\right), \quad (6.1)$$

with some constant C . (The terms $\sim \Lambda^2$ and $\sim \ln(\Lambda)$ are removed by renormalization.)

Apart from working with finite Λ it is also necessary to introduce two numerical parameters, the box size R and the maximum momentum P_{max} (see app. B), in order to obtain a finite basis for the diagonalization of \mathcal{H} . For a fixed value of Λ both have to be taken large enough so that $E_{sea}^{ren}(\Lambda)$ does not change any more when they are further increased. In Tab. 1 we plot results for fixed $m_F = 2m_W$, $N_{CS} = 0.5$ and $\Lambda = 5m_W$ for different R and P_{max} . It can be seen that stability is reached for $R \approx 12m_W^{-1}$ and $P_{max} \approx 3\Lambda$ so that we obtain as our result:

$$E_{sea}^{ren}(\Lambda = 5m_W, m_F = 2m_W, N_{CS} = 0.5) = 8.55m_W, \quad (6.2)$$

P_{max}/Λ	1.5	2.0	2.5	3.0	3.5
$R m_W = 5$	7.98	7.29	7.20	7.20	7.20
$R m_W = 7$	8.99	8.34	8.25	8.25	8.25
$R m_W = 9$	9.25	8.57	8.49	8.48	8.48
$R m_W = 10$	9.25	8.61	8.52	8.52	8.52
$R m_W = 11$	9.28	8.62	8.54	8.54	8.54
$R m_W = 12$	9.31	8.64	8.55	8.55	8.55
$R m_W = 13$	9.31	8.64	8.55	8.55	8.55
$R m_W = 14$	9.28	8.64	8.55	8.55	8.55

Table 1: $E_{sea}^{ren}(\Lambda = 5 m_W)$ for different values of the numerical parameters R and P_{max} with $m_F = 2 m_W$, $N_{CS} = 0.5$ and $\Lambda = 5 m_W$ fixed. Stability is reached at $R \approx 12 m_W^{-1}$ and $P_{max} \approx 3 \Lambda$.

with a numerical error of less than 0.2 %. Using the same method we obtain results for other values of Λ and for different m_F and N_{CS} . It turns out that in general it is sufficient to choose $R = 12 m_W^{-1}$ and $P_{max} = 3.5 \Lambda$. In Tab. 2 we present results for various values of Λ with $R = 12 m_W^{-1}$ fixed. Additionally we have written values for $E_{sea}^{ren}(\Lambda)$ obtained from eq. (6.1) with $E_{sea}^{ren}(\infty) = 9.09 m_W$ and $C = 13.54 m_W^3$ into the last column. A comparison with the

P_{max}/Λ	1.5	2.0	2.5	3.0	3.5	from eq. (6.1)
$\Lambda/m_W = 3$	8.28	7.71	7.64	7.63	7.63	7.59
$\Lambda/m_W = 4$	8.86	8.33	8.25	8.25	8.25	8.24
$\Lambda/m_W = 5$	9.27	8.63	8.55	8.55	8.55	8.55
$\Lambda/m_W = 6$	9.54	8.80	8.71	8.71	8.71	8.71
$\Lambda/m_W = 8$	9.89	8.98	8.88	8.88	8.88	8.88

Table 2: $E_{sea}^{ren}(\Lambda)$ for various values of Λ and P_{max} . $R = 12 m_W^{-1}$, $m_F = 2 m_W$ and $N_{CS} = 0.5$ are fixed. The values in the last column are obtained by eq. (6.1) with $E_{sea}^{ren}(\infty) = 9.09 m_W$ and $C = 13.54 m_W^3$.

numerical results shows that the power law eq. (6.1) is fulfilled very accurately. Therefore the numerical error of the extrapolated value $E_{sea}^{ren}(\infty)$ is of the same

order as the error of $E_{sea}^{ren}(\Lambda)$ for finite Λ . Thus our extrapolated result for E_{sea}^{ren} finally reads:

$$E_{sea}^{ren}(m_F = 2m_W, N_{CS} = 0.5) = 9.09 m_W, \quad (6.3)$$

again with a numerical error of 0.2 %. Our results for different values of m_F and N_{CS} were obtained the same way. The numerical errors always have roughly the same size. The relative error can increase up to 2% for small m_F where E_{sea}^{ren} is considerably lower than for $m_F = 2m_W$. This accuracy is fully sufficient for our purpose; one should keep in mind that the error arising from taking equal masses for the top and bottom quark is surely bigger than the numerical error.

In Fig. 3 we have plotted $E_{fer}^{ren} \equiv E_{sea}^{ren} + \varepsilon_{val} \theta(\varepsilon_{val})$ as a function of N_{CS} for $m_F/m_W = 0, 1$ and 2 . For $m_F = 0$ there is no contribution from the valence level, the energy is symmetric with respect to $N_{CS} = 0.5$. Its total value is very small ($E_{sea}^{ren} = 0.18 m_W$ for $N_{CS} = 0.5$) compared to the classical energy of the boson fields ($\approx 100 m_W$ for $N_{CS} = 0.5$). This is also the case for $m_F = m_W$, where the energy is the sum of the symmetric sea and antisymmetric valence part. The fermionic energy E_{fer}^{ren} is only significant in comparison to the classical energy when m_F is much larger than m_W . For $m_F = 2m_W$ the energy of the fermions is already about 9% of the classical energy, and it increases dramatically with m_F . In fact, one can show that in the leading order the sea energy grows with m_F as $m_F^4 \ln(m_F)$. This law is already a good approximation for $m_F \geq 3m_W$. In Tab. 3 we have plotted results of E_{sea}^{ren} for different m_F at $N_{CS} = 0.5$.

m_F/m_W	0	1	2	3	4	5	6
E_{sea}^{ren}/m_W	0.18	0.51	9.05	72.63	303.5	862	2001

Table 3: E_{sea}^{ren} as a function of m_F for fixed $N_{CS} = 0.5$. The energy increases according to $E_{sea}^{ren} \sim m_F^4 \ln(m_F)$. It should be compared to the classical energy which is about $100 m_W$ for $N_{CS} = 0.5$.

Before we turn to the discussion of the temperature dependent contribution E_{fer}^{temp} to the sphaleron transition rate and the baryon number and -density, let us briefly comment on the numerical accuracy of these UV-finite quantities. The only parameters which turn up in the numerical evaluation are R and P_{max} . Again, both have to be chosen large enough to ensure stability of the results.

This is done in analogy to the method for the calculation of $E_{sea}^{ren}(\Lambda)$ for fixed Λ . The numerical errors are again in the range of 1% to 2%.

We are now going to present the temperature dependent contributions to the sphaleron transition rate, given by eqs. (5.19–5.21). In this paper we only considered the classical term βE_{class}^{ren} and the fermionic part βE_{fer}^{temp} but not the bosonic part βE_{bos}^{temp} . The temperature enters the transition rate in three ways: First, in form of the prefactor $\beta = 1/T$ which causes the transition rate to become unsuppressed when $E_{tot}(T) \sim T$. Second, the masses get renormalized via eq. (5.16) so that the energy $E_{tot}(T)$ is roughly proportional to $v(T)/v(0)$ given by eq. (5.15). Third, the last term of E_{fer}^{temp} is explicitly dependent on β . The first two effects are numerically trivial but very large, while the last one is difficult to compute and rather small.

We start by considering the first two aspects. The dominant contribution in eq. (5.20) is

$$\beta E_{class}^{ren}(T) = \frac{1}{T} E_{class}^{ren}(0) \left(1 - \frac{3m_H^2 + 9m_W^2 + 4 \sum_{\text{doubl.}} m_F^2}{6v^2 m_H^2} T^2 \right). \quad (6.4)$$

For $T \rightarrow 0$ this terms goes to infinity, but it decreases rapidly with increasing T . In the vicinity of the critical temperature

$$T_c^2 = \frac{6v^2 m_H^2}{3m_H^2 + 9m_W^2 + 4 \sum_{\text{doubl.}} m_F^2}, \quad (6.5)$$

where the symmetry breaking of electroweak theory and the sphaleron barrier disappear the function $\beta E_{class}^{ren}(T)$ goes to zero and the baryon number violation rate becomes unsuppressed.

The value of T_c and the quantitative behaviour of $\beta E_{class}^{ren}(T)$ depend largely on the choice of the parameters. We wish to focus our interest to a situation which resembles the physical one as close as possible. As it was mentioned above to preserve spherical symmetry of the Dirac equation one has to consider the case of equal masses for up and down fermions. This approximation is not so good for the three (t, b) doublets. In the case $m_{t,b} < m_W$ the fermionic corrections can be estimated using the average mass of the doublet, and treating the difference as a perturbation. The corrections are anyhow small in this case. In the more realistic case $m_b \ll m_W \ll m_t$ the correction from the top quark is *half* that of the doublet with both masses equal to m_t (This recipe can easily be derived from eqs. (4.5) and (5.12) in the limit $m_t \gg m_W$). Therefore, in our numerical estimates we take 9+3/2 massless fermion doublets and 3/2 massive

doublets with mass m_t which we vary in the range $m_t/m_W = 1.5, 2.0, 2.5$. In particular the sums in eqs. (6.4, 6.5) are replaced by $3/2 m_t^2$.

We have plotted $\beta E_{class}^{ren}(T)$ as a function of T in Fig. 4 (dashed lines) for the masses $m_t/m_W = 1.5, 2.0$ and 2.5 . We realize that T_c is rather low (between m_W and $1.5 m_W$). One can obtain a higher T_c by taking a larger Higgs mass, but this will not change the picture qualitatively. The current experimental bounds do not suggest that m_H should be considerably higher than m_W . We have already stated in Section 5 that the range of applicability of the Langer–Affleck formula is roughly given by $0.3 m_W \approx \omega_-/2\pi \leq T \leq T_c \approx 1.5 m_W$. This is the range we use in Fig. 4, but one has to be careful if T is very close to T_c . In this case the Langer–Affleck formula is clearly not valid because the barrier gets so low that the transition occurs far above the sphaleron.

We now want to investigate how far the fermionic fluctuations βE_{fer}^{temp} of eq. (5.21) influence the transition rate. The numerical results for this contribution are included in Fig. 4 (solid lines), again for the three choices $m_t/m_W = 1.5, 2.0$ and 2.5 . We find that the results for these cases are quite different. For $m_t = 2.5 m_W$ and $T \approx 0.5 m_W$ the fermionic fluctuations increase the exponent of the classical Boltzmann factor by about 50%. For $T \approx 0.9 m_W$ this increase is even about 65%. On the other hand, for $m_t = 1.5 m_W$ the fluctuations are only between 5 and 9% of the classical exponent. We conclude that the fermion loops suppress the baryon number violation rate in any case, but the strength of the suppression depends on the value for the mass of the top quark. We expect that the above numbers slightly change if the difference between m_t and m_b is treated perturbatively in higher orders.

The suppression of the transition rate is important for the understanding of the matter excess in the universe. However, such cosmological consequences are still a matter of discussion (see e.g. [9, 10]), and we will not go into details here.

Let us turn to the discussion of the baryon number and -density. First we have to find reasonable definitions for these quantities. In principle, the baryon number is the number of all negative energy eigenstates of the Dirac Hamiltonian, relative to the vacuum. The valence state always contributes to the baryon number, so it has to be added explicitly after it has crossed zero. However, the increase of the baryon number according to the law $B = N_{CS}$ is not only caused by the level crossing of the valence state, but it is also due to a process that happens at both ends of the spectrum. To see this let us return

to Fig. 2 which demonstrates that, going from $N_{CS} = 0$ to $N_{CS} = 1$, one state emerges from "outside the spectrum" and joins the negative continuum, and another one disappears "from the positive continuum to infinity". In order to take this effect into account correctly we have to introduce a regularization and compute the result with a finite cut-off which eventually must be sent to infinity. Thus we define:

$$\begin{aligned}
B &= \lim_{\Lambda \rightarrow \infty} \left\{ N(\varepsilon_\lambda < 0) - N(\varepsilon_\lambda^{(0)} < 0) \right\}_{reg} + \theta(\varepsilon_{val}) \\
&= \lim_{\Lambda \rightarrow \infty} \left\{ -\frac{1}{2} \sum_\lambda \text{sign}(\varepsilon_\lambda) \right\}_{reg} + \theta(\varepsilon_{val}) \\
&= \lim_{\Lambda \rightarrow \infty} \left\{ - \sum_\lambda \frac{\varepsilon_\lambda}{2\sqrt{\pi}} \int_{\frac{1}{\Lambda^2}}^\infty dt t^{-1/2} e^{-\varepsilon_\lambda^2 t} \right\} + \theta(\varepsilon_{val}). \quad (6.6)
\end{aligned}$$

It is possible to show analytically that $\delta B = \delta N_{CS}$ with N_{CS} and B being defined by eq. (2.1) and eq. (6.6), respectively. Here "δ" means the variation with respect to the boson fields. One has to differentiate the integral in eq. (6.6) with respect to ε_λ , perform the t integral and expand in powers of $1/\Lambda$. The only term which does not vanish in the limit $\Lambda \rightarrow \infty$ is identical to δN_{CS} . For the baryon density we obtain:

$$\begin{aligned}
\rho(r) &= \lim_{\Lambda \rightarrow \infty} \int d\Omega \sum_\lambda \varphi_\lambda^\dagger(\mathbf{r}) \varphi_\lambda(\mathbf{r}) \left[-\frac{\varepsilon_\lambda}{2\sqrt{\pi}} \int_{\frac{1}{\Lambda^2}}^\infty dt t^{-1/2} e^{-\varepsilon_\lambda^2 t} \right] \\
&\quad + \theta(\varepsilon_{val}) \int d\Omega \varphi_{val}^\dagger(\mathbf{r}) \varphi_{val}(\mathbf{r}). \quad (6.7)
\end{aligned}$$

Here $\varphi_\lambda(\mathbf{r})$ are the eigenfunctions of the Dirac Hamiltonian: $\mathcal{H}\varphi_\lambda = \varepsilon_\lambda \varphi_\lambda$. Of course, by definition we have $B = \int_0^\infty dr r^2 \rho(r)$.

In order to evaluate eqs. (6.6, 6.7) numerically we have to insert the eigenvalues ε_λ obtained from the diagonalization in different sectors of grand spin K . It turns out that B and ρ are dominated by the $K = 0$ sector. In fact, its contribution is usually more than 90% of the total value. This means that the created baryon is basically in a $K = 0$ state.

In Tab. 4 we present the baryon number B as a function of N_{CS} for $m_F = m_W$. We observe that the law $B = N_{CS}$ is excellently reproduced. The same behaviour is obtained for different masses m_F . The baryon density as a function of the radial distance r is plotted in Fig. 5 for $N_{CS} = 0.26, 0.5, 0.74$ and close to 1 ($m_F = m_W$). Between $N_{CS} = 0$ and $N_{CS} = 0.5$ the density increases with N_{CS} for each fixed r . For $N_{CS} > 0.5$ the density at the origin $\rho(0)$

N_{CS}	0.00	0.15	0.26	0.35	0.43	0.50	0.57	0.65	0.74	0.85	1.00
B	0.00	0.18	0.27	0.35	0.43	0.50	0.57	0.65	0.73	0.82	1.00

Table 4: B as a function of N_{CS} for $m_F = m_W$. The data confirm the law $B = N_{CS}$ coming from the anomaly.

decreases again, while the integral B is still increasing (as seen from Tab. 4). Thus we are creating a baryon which becomes more and more delocalized. Approaching $N_{CS} = 1$ the density becomes independent of r and infinitesimally small everywhere. This corresponds to a free, unbound particle as expected from a vacuum configuration of the classical fields.

Finally we have checked the influence of the Higgs mass m_H on the preceding results. Qualitatively, the picture was found to be the same for any m_H (at very large m_H , however, the sphaleron solution becomes modified, see [14]). In fact, we observe that both E_{fer}^{ren} and E_{fer}^{temp} are slightly decreasing functions of m_H . So for $m_H > m_W$ they always have the same order of magnitude as their classical counterparts. Only for the unphysical value $m_H \rightarrow 0$ the fermionic terms show a significant increase. In this case the energy E_{fer}^{ren} reaches approximately 10% of the classical energy ($m_F = m_W$), which is about 20 times higher than for $m_H = m_W$. This relatively large value is due to the slow decrease of the boson fields for $r \rightarrow \infty$ which causes a strong perturbation of the Dirac sea.

Acknowledgement: We are grateful to V.Petrov and P.Pobylitsa for numerous discussions. D.D. and M.P. would like to thank the Institute for Theoretical Physics II of the Ruhr Universität Bochum for hospitality. Their work was sponsored in part by the Russian Foundation for Fundamental Research under grant #93-02-3858 and by the Deutsche Forschungsgemeinschaft.

Appendix A

For the sake of completeness we cite the eqs. for getting the minimal-energy configurations of Akiba *et al.* [13]. They are found from the Euler–Lagrange eqs. which follow from varying eq. (2.8):

$$A'' = \frac{1}{x^2} A(A^2 + B^2 - 1) + A(H^2 + G^2) + G^2 - H^2 - 2\zeta B',$$

$$\begin{aligned}
B'' &= \frac{1}{x^2} B(A^2 + B^2 - 1) + B(H^2 + G^2) - 2HG + 2\zeta A', \\
(xH)'' &= \frac{1}{2x} H[(A-1)^2 + B^2] - \frac{1}{x} BG + \frac{\kappa^2}{2} xH(H^2 + G^2 - 1), \\
(xG)'' &= \frac{1}{2x} G[(A-1)^2 + B^2] + \frac{2}{x} AG - \frac{1}{x} BH + \frac{\kappa^2}{2} xG(H^2 + G^2 - 1).
\end{aligned} \tag{A.1}$$

A consequence of these eqs. is a "conservation law" which can be used to check the accuracy of the numerical integration:

$$(AB' - A'B) + x^2(HG' - H'G) + \zeta(1 - A^2 - B^2) = 0. \tag{A.2}$$

The boundary conditions for eqs. (A.1) follow from the requirement that there are no singularities at the origin and that the energy functional does not diverge at infinity. The first requirement implies the following behaviour of the functions near the origin:

$$\begin{aligned}
A &= \cos \alpha (1 + rx^2) - \frac{1}{3}(st + 2r\zeta)(\sin \alpha) x^3 + \dots, \\
B &= \sin \alpha (1 + rx^2) + \frac{1}{3}(st + 2r\zeta)(\cos \alpha) x^3 + \dots, \\
H &= s \cos \frac{\alpha}{2} + t(\sin \frac{\alpha}{2}) x + \frac{1}{12}\kappa^2 s(s^2 - 1)(\cos \frac{\alpha}{2}) x^2 + \dots, \\
G &= s \sin \frac{\alpha}{2} - t(\cos \frac{\alpha}{2}) x + \frac{1}{12}\kappa^2 s(s^2 - 1)(\sin \frac{\alpha}{2}) x^2 + \dots,
\end{aligned} \tag{A.3}$$

where α, r, s, t are arbitrary constants.

Requiring the convergence of the energy integral at infinity and solving the eqs. (A.1) at large x one gets the following behaviour of the functions at $x \rightarrow \infty$:

$$\begin{aligned}
A &= \cos \gamma + e \sin(\zeta x + \beta) E(x), \\
B &= \sin \gamma - e \cos(\zeta x + \beta) E(x), \\
H &= \cos \frac{\gamma}{2} \left(1 + \frac{h}{x} e^{-\kappa x}\right) - e \sin \frac{\gamma}{2} \cos(\zeta x + \beta - \gamma + \delta) \frac{E(x)}{x^2}, \\
G &= \sin \frac{\gamma}{2} \left(1 + \frac{h}{x} e^{-\kappa x}\right) + e \cos \frac{\gamma}{2} \cos(\zeta x + \beta - \gamma + \delta) \frac{E(x)}{x^2},
\end{aligned} \tag{A.4}$$

where we have denoted

$$E(x) \equiv \exp \left(-\sqrt{1 - \zeta^2} x \right), \quad \zeta = \sin \frac{\delta}{2}, \quad \sqrt{1 - \zeta^2} = \cos \frac{\delta}{2}, \tag{A.5}$$

and γ, β, e and h are arbitrary constants.

Note that the asymptotics (A.4) is valid only if $m_H \sim m_W$; if the Higgs is much heavier than the W boson, eqs. (A.4) have to be modified.

We have thus four arbitrary constants defining the behaviour of the functions at infinity (β, γ, e, h) and four in the origin (α, r, s, t) . Matching solutions of eqs. (A.1) starting from the origin with those starting from infinity, one finds these constants for a given value of ζ (and κ) – up to a global gauge rotation, however. The point is, only the combination $\gamma - \alpha$ is invariant under the gauge rotation (2.6) with a constant P . One can use this freedom to fix $\alpha = 0$, for example.

It should be noticed that eqs. (A.1) have a solution only for $|\zeta| < 1$. The end points of this interval correspond to $N_{CS} = 0, 1$; it is seen from eqs. (A.4, A.5) that at $|\zeta| \rightarrow 1$ the functions rather oscillate than decrease.

Appendix B

In this appendix we summarize how the Dirac Hamiltonian \mathcal{H} of eq. (3.7) is diagonalized. Since it commutes with the grand spin operator $\hat{\mathbf{K}}$, we diagonalize it in a basis of eigenfunctions of $\hat{\mathbf{K}}^2$ and \hat{K}_3 . To this end we introduce normalized eigenstates of the commuting operators $\hat{\mathbf{L}}^2, \hat{\mathbf{J}}^2 = (\hat{\mathbf{L}} + \hat{\mathbf{S}})^2, \hat{\mathbf{K}}^2 = (\hat{\mathbf{J}} + \hat{\mathbf{T}})^2$ and its third component \hat{K}_3 . Naturally, they are also eigenstates of the operators $\hat{\mathbf{S}}^2 = \hat{\mathbf{T}}^2 = 3/4$. We shall use the short-hand notation $|K, J, L; K_3\rangle$ to denote these states.

Since only the operators $\hat{\mathbf{K}}^2, \hat{K}_3$ commute with the Hamiltonian \mathcal{H} but not $\hat{\mathbf{J}}^2$ or $\hat{\mathbf{L}}^2$, states labelled by different J, L at given K, K_3 will mix in the eigenvalue eq. (3.6). Generally speaking, for given values of K, K_3 the following four states mix:

$$\begin{aligned} & |K, K + \frac{1}{2}, K + 1; K_3\rangle, \quad |K, K + \frac{1}{2}, K; K_3\rangle, \\ & |K, K - \frac{1}{2}, K; K_3\rangle, \quad |K, K - \frac{1}{2}, K - 1; K_3\rangle. \end{aligned} \quad (\text{B.1})$$

We therefore have to decompose the spinor-isospinor functions $\tilde{\psi}_L, \tilde{\chi}_R$ in the above four states for every value of K, K_3 :

$$\begin{aligned} \tilde{\psi}_L(\mathbf{r}) &= \sum_{K=0}^{\infty} \sum_{K_3=-K}^K \sum_{J=K-\frac{1}{2}}^{K+\frac{1}{2}} \sum_{L=J-\frac{1}{2}}^{J+\frac{1}{2}} i^L f_{JL}^{KK_3}(r) \langle \Omega | K, J, L; K_3 \rangle, \\ \tilde{\chi}_R(\mathbf{r}) &= \sum_{K=0}^{\infty} \sum_{K_3=-K}^K \sum_{J=K-\frac{1}{2}}^{K+\frac{1}{2}} \sum_{L=J-\frac{1}{2}}^{J+\frac{1}{2}} i^L g_{JL}^{KK_3}(r) \langle \Omega | K, J, L; K_3 \rangle. \end{aligned} \quad (\text{B.2})$$

The eigenvalue eq. (3.6) is thus mixing four functions f (from $\tilde{\psi}_L$) and four functions g (from $\tilde{\chi}_R$) for any value of K, K_3 . Since the Hamiltonian is block-diagonal with respect to K_3 , eq. (3.6) results in a system of eight ordinary differential eqs. for eight independent functions for each K . In the case of $K = 0$ where the last two states in eq. (B.1) are absent, only two states for $\tilde{\psi}_L$ and two for $\tilde{\chi}_R$ mix, and the eigenvalue equation involves only four functions. This particular case was considered recently in ref. [16].

The set of differential equations will be solved by putting the system into a large but finite spherical box. To insure that at the boundaries of the box the boson fields take their vacuum values, we have to switch to a gauge in which $A(\infty) = 1, B(\infty) = 0, C(\infty) = 0, H(\infty) = 1$ and $G(\infty) = 0$. Moreover, to insure continuity at the origin the values of the fields at $r = 0$ must be $A(0) = 1, B(0) = 0, C(0) = 0$ and $G(0) = 0$. Therefore we have to give up the simplifying choice $C(r) \equiv 0$ and to include the C -field into the formulae. This is, however, no substantial difficulty.

In substituting the decomposition (B.2) into eq. (3.6) one has to calculate matrix elements in the $|K, J, L; K_3\rangle$ basis of the scalar operators appearing in eq. (3.6), namely $(\alpha\mathbf{e}\mathbf{n}), (\alpha\phi), (\phi\mathbf{n}), (\alpha\partial), ([\alpha\mathbf{e}\times\phi]\mathbf{n})$ and $(\alpha\mathbf{e}\mathbf{n})(\phi\mathbf{n})$. We call these operators "scalar" as they commute with the operator $\hat{\mathbf{K}}^2$, hence equations for different K will not be mixed.

Thus, the Dirac Hamiltonian (3.7) is block-diagonal in the $|K, J, L; K_3\rangle$ basis, where the blocks correspond to sectors with definite K and K_3 ; we call these blocks \mathcal{H}_{KK_3} . Since they do not depend on K_3 this index will be suppressed subsequently. Each \mathcal{H}_K is a 8×8 matrix acting on an 8-vector V_K :

$$\mathcal{H}_K V_K = E V_K, \quad (\text{B.3})$$

where

$$V_K = \begin{pmatrix} f_{K+\frac{1}{2}, K+1}, & f_{K+\frac{1}{2}, K}, & f_{K-\frac{1}{2}, K}, & f_{K-\frac{1}{2}, K-1}, \\ g_{K+\frac{1}{2}, K+1}, & g_{K+\frac{1}{2}, K}, & g_{K-\frac{1}{2}, K}, & g_{K-\frac{1}{2}, K-1} \end{pmatrix}, \quad (\text{B.4})$$

and \mathcal{H}_K can be presented as

$$\mathcal{H}_K = \begin{pmatrix} \mathcal{D}_K + \mathcal{V}_K & \mathcal{W}_K \\ \mathcal{W}_K^\dagger & -\mathcal{D}_K \end{pmatrix}. \quad (\text{B.5})$$

Here \mathcal{D}_K is a 4×4 matrix composed of differentiation operators:

$$\mathcal{D}_K = \begin{pmatrix} 0 & -\frac{d}{dx} + \frac{K}{x} & 0 & 0 \\ \frac{d}{dx} + \frac{K+2}{x} & 0 & 0 & 0 \\ 0 & 0 & 0 & -\frac{d}{dx} + \frac{K-1}{x} \\ 0 & 0 & \frac{d}{dx} + \frac{K+1}{x} & 0 \end{pmatrix}, \quad (\text{B.6})$$

while \mathcal{V}_K and \mathcal{W}_K are also 4×4 matrices made of the background W and H fields. To shorten notations we introduce

$$\begin{aligned} b_K &= \sqrt{K(K+1)}, \quad c_K = 2K+1, \\ A_K &= \frac{1-A(x)}{xc_K}, \quad B_K = \frac{B(x)}{xc_K}, \quad C_K = \frac{C(x)}{xc_K}, \quad G_K = \frac{G(x)}{c_K}, \quad H_K = H(x). \end{aligned} \quad (\text{B.7})$$

Using standard $6j$ symbols as described in app. C, we obtain for the matrix \mathcal{V}_K :

$$\begin{pmatrix} B_K(K+1) - \frac{C_K}{2} & -A_K(K+1) & A_K b_K & (B_K - C_K)b_K \\ -A_K(K+1) & -B_K(K+1) - \frac{C_K}{2} & (B_K + C_K)b_K & -A_K b_K \\ A_K b_K & (B_K + C_K)b_K & -B_K K + \frac{C_K}{2} & A_K K \\ (B_K - C_K)b_K & -A_K b_K & A_K K & B_K K + \frac{C_K}{2} \end{pmatrix} \quad (\text{B.8})$$

and

$$\mathcal{W}_K = m_F \begin{pmatrix} H_K & G_K & -2G_K b_K & 0 \\ -G_K & H_K & 0 & -2G_K b_K \\ 2G_K b_K & 0 & H_K & -G_K \\ 0 & 2G_K b_K & G_K & H_K \end{pmatrix}. \quad (\text{B.9})$$

In eqs. (B.3–B.9) we imply that x is the distance from the origin measured in units of m_W^{-1} ; the energy eigenvalues E and the fermion mass m_F are measured in units of m_W .

For $K = 0$ eqs. (B.3–B.9) reduce to those derived in ref. [16]; for any K but $A = B = 0$ we get to the equations derived in a different context in ref. [31].

In order to find the Dirac eigenvalues numerically one can use various methods. One method [31] is to express fermionic observables (such as the energy of the Dirac sea, etc.) through the phase shifts of the Hamiltonian \mathcal{H}_K . In this work we shall use an alternative method: the diagonalization of the Hamiltonian \mathcal{H}_K (B.5) in the so-called Kahana–Ripka basis [32]. This method was previously used in the chiral nucleon model [33]. The idea is to discretize the spectrum by putting the fermions into a large spherical box, and diagonalizing

the Hamiltonian in the basis of spherical Bessel functions which are eigenfunctions of the zero-field Hamiltonian. We will now introduce this technique.

In the absence of the background field we have $A(x) = 1$, $B(x) = 0$, $C(x) = 0$, $H(x) = 1$ and $G(x) = 0$, therefore $\mathcal{V}_K = 0$, $\mathcal{W}_K = m_F$, so that the free Hamiltonian becomes

$$\mathcal{H}_K^{(0)} = \begin{pmatrix} \mathcal{D}_K & m_F \\ m_F & -\mathcal{D}_K \end{pmatrix}, \quad (\text{B.10})$$

and the eigenvalue equation can be easily solved analytically. For given grand spin K and momentum p we find, generally speaking, eight linearly independent solutions of eq. (B.3), which we call $v_K^{(q)}$, $q = 1 \dots 8$; each of them is an 8-vector in the sense of eq. (B.4). Introducing a column composed of the spherical Bessel functions,

$$J_{K,i} = \begin{pmatrix} j_{K+1}(px), & j_K(px), & j_K(px), & j_{K-1}(px), \\ j_{K+1}(px), & j_K(px), & j_K(px), & j_{K-1}(px) \end{pmatrix}, \quad i = 1 \dots 8, \quad (\text{B.11})$$

the eight solutions of the free eigenvalue equation can be written as

$$v_{K,i}^{(r)} = \mathcal{N} C_i^{(r)} J_{K,i} \quad (\text{no summation in } i!), \quad (\text{B.12})$$

where \mathcal{N} is the normalization factor (see below). With $\varepsilon \equiv \sqrt{p^2 + m_F^2}$, the factors $C_i^{(r)}$ are given by

$$\begin{aligned} C_i^{(1)} &= \frac{1}{\sqrt{2}} \left(\frac{m_F}{\varepsilon}, 0, 0, 0, 1, -\frac{p}{\varepsilon}, 0, 0 \right), & C_i^{(5)} &= \frac{1}{\sqrt{2}} \left(-\frac{m_F}{\varepsilon}, 0, 0, 0, 1, \frac{p}{\varepsilon}, 0, 0 \right), \\ C_i^{(2)} &= \frac{1}{\sqrt{2}} \left(-\frac{p}{\varepsilon}, -1, 0, 0, 0, -\frac{m_F}{\varepsilon}, 0, 0 \right), & C_i^{(6)} &= \frac{1}{\sqrt{2}} \left(\frac{p}{\varepsilon}, -1, 0, 0, 0, \frac{m_F}{\varepsilon}, 0, 0 \right), \\ C_i^{(3)} &= \frac{1}{\sqrt{2}} \left(0, 0, \frac{m_F}{\varepsilon}, 0, 0, 0, 1, -\frac{p}{\varepsilon} \right), & C_i^{(7)} &= \frac{1}{\sqrt{2}} \left(0, 0, -\frac{m_F}{\varepsilon}, 0, 0, 0, 1, \frac{p}{\varepsilon} \right), \\ C_i^{(4)} &= \frac{1}{\sqrt{2}} \left(0, 0, -\frac{p}{\varepsilon}, -1, 0, 0, 0, -\frac{m_F}{\varepsilon} \right), & C_i^{(8)} &= \frac{1}{\sqrt{2}} \left(0, 0, \frac{p}{\varepsilon}, -1, 0, 0, 0, \frac{m_F}{\varepsilon} \right). \end{aligned} \quad (\text{B.13})$$

It is convenient to discretize the free Dirac spectrum by the following trick [32, 33] which preserves the spherical symmetry of the problem and makes the eight states $v_K^{(r)}$ orthogonal to each other and to any other states with different K and ε . Namely, we introduce a large radius R (eventually to be taken to infinity) and fix the spectrum for given K as zeros of the spherical Bessel function:

$$j_K(p_n R) = 0. \quad (\text{B.14})$$

If $\alpha_{m,n}$ are zeros of $j_K(z)$ one has the following ortho-normalization conditions:

$$\begin{aligned} & \int_0^1 dt t^2 j_K(\alpha_m t) j_K(\alpha_n t) \\ &= \int_0^1 dt t^2 j_{K\pm 1}(\alpha_m t) j_{K\pm 1}(\alpha_n t) = \delta_{mn} \frac{1}{2} [j_{K\pm 1}(\alpha_n)]^2. \end{aligned} \quad (\text{B.15})$$

These relations provide the orthogonality of the eight degenerate states (B.12) as well as their orthogonality to states with different p_n at given K . States with different values of K are orthogonal owing to the angular integration. From eq. (B.15) we also learn that the normalization factor \mathcal{N} in eq. (B.12) is

$$\mathcal{N} = \sqrt{\frac{2}{R^3}} |j_{K\pm 1}(p_n R)|^{-1}. \quad (\text{B.16})$$

We have thus constructed a complete ortho-normalized set of states $v_K^{(q)}(p_n)$ (given by eqs. (B.11–B.13)) which are the eigenfunctions of the free Dirac operator.

The eigenstates of the full Dirac Hamiltonian (B.5) can be now found from a direct diagonalization of the matrix

$$\mathcal{H}_K^{rs}(p_m, p_n) = \int_0^R dx x^2 v_{K,i}^{(r)}(p_m, x) \mathcal{H}_{K,ij} v_{K,j}^{(s)}(p_n, x) \quad (\text{B.17})$$

(summation over $i, j = 1 \dots 8$ is assumed here). The superscripts r, s run over $1 \dots 8$ while the radial momenta $p_{m,n}$ are given by eq. (B.14). They vary from small values of the order of $1/R$ up to some numerical cut-off P_{max} , which ensures the finiteness of the basis. P_{max} and R have to be taken large enough so that no result changes when they are further increased.

Appendix C

In this appendix we derive matrix elements of scalar operators entering the Hamiltonians for bosonic and fermionic fluctuations about the spherically symmetric sphaleron. These operators commute with the grand spin

$$\hat{\mathbf{K}} = \hat{\mathbf{J}} + \hat{\mathbf{T}} = \hat{\mathbf{L}} + \hat{\mathbf{S}} + \hat{\mathbf{T}}. \quad (\text{C.1})$$

The fully normalized set of states in this momentum-adding scheme is

$$|L, S, [J], T, K, K_3\rangle = \sum_{L_3, S_3, J_3, T_3} C_{JJ_3, TT_3}^{KK_3} C_{LL_3, SS_3}^{JJ_3} |SS_3\rangle |TT_3\rangle |LL_3\rangle. \quad (\text{C.2})$$

These states are the eigenfunctions of the operators $\hat{\mathbf{K}}^2$, $\hat{\mathbf{K}}_3$, $\hat{\mathbf{L}}^2$, $\hat{\mathbf{S}}^2$, $\hat{\mathbf{J}}^2$ and $\hat{\mathbf{T}}^2$. On general grounds one can show that such Hamiltonians depend on the following operators which commute with the grand spin:

$$\hat{\mathbf{J}}^2, \hat{\mathbf{L}}^2, \hat{\mathbf{T}}^2, \hat{\mathbf{S}}^2, \hat{\mathbf{S}} \cdot \hat{\mathbf{L}}, \hat{\mathbf{S}} \cdot \hat{\mathbf{T}}, \hat{\mathbf{T}} \cdot \hat{\mathbf{n}}, \hat{\mathbf{S}} \cdot \hat{\mathbf{n}}, \hat{\mathbf{T}} \cdot [\hat{\mathbf{S}} \times \hat{\mathbf{n}}], \hat{\mathbf{T}} \cdot [\hat{\mathbf{n}} \times \hat{\mathbf{L}}], \quad (\text{C.3})$$

where $\hat{\mathbf{n}} = \hat{\mathbf{x}}/|\hat{\mathbf{x}}|$. We use the general relations

$$\partial_k = n_k \frac{\partial}{\partial r} - \frac{i}{r} \varepsilon_{klm} n_l L_m, \quad L_j = -i \varepsilon_{jlm} x_l \partial_m. \quad (\text{C.4})$$

Any scalar operator commuting with the grand spin can be expressed through the set of operators (C.3), for example

$$\hat{\mathbf{T}} \cdot \hat{\mathbf{L}} = \frac{1}{2} (\hat{\mathbf{K}}^2 - \hat{\mathbf{J}}^2 - \hat{\mathbf{T}}^2) - \hat{\mathbf{S}} \cdot \hat{\mathbf{T}} \quad \text{or} \quad \hat{\mathbf{S}} \cdot \hat{\mathbf{L}} = \frac{1}{2} (\hat{\mathbf{J}}^2 - \hat{\mathbf{S}}^2 - \hat{\mathbf{L}}^2). \quad (\text{C.5})$$

To calculate matrix elements of the operators (C.3) in the basis (C.2) we use the technique of irreducible tensor operators and the Wigner–Eckart theorem (for details see [34]).

We illustrate this technique by calculating the complicated matrix element $\langle L', S', [J'], T', K, K_3 | \hat{\mathbf{T}} \cdot (\hat{\mathbf{S}} \times \hat{\mathbf{n}}) | L, S, [J], T, K, K_3 \rangle$. The operator $\hat{\mathbf{T}}$ does not act on the spin and angular variables so that the matrix element can be factorized as

$$\begin{aligned} & \langle L', S', [J'], T', K, K_3 | \hat{\mathbf{T}} \cdot (\hat{\mathbf{S}} \times \hat{\mathbf{n}}) | L, S, [J], T, K, K_3 \rangle \\ &= (-1)^{J+T'+K} \left\{ \begin{array}{ccc} K & T' & J' \\ 1 & J & T \end{array} \right\} \langle L' S' [J'] \parallel \hat{\mathbf{S}} \times \hat{\mathbf{n}} \parallel L S [J] \rangle \langle T' \parallel \hat{\mathbf{T}} \parallel T \rangle, \end{aligned} \quad (\text{C.6})$$

where

$$\langle T' \parallel \hat{\mathbf{T}} \parallel T \rangle = \sqrt{T(T+1)(2T+1)} \delta_{TT'}. \quad (\text{C.7})$$

The spin operator $\hat{\mathbf{S}}$ acts only on spin variables whereas $\hat{\mathbf{n}}$ acts on angular variables, so one can again factorize the matrix element as

$$\begin{aligned} & \langle L' S' [J'] \parallel \hat{\mathbf{S}} \times \hat{\mathbf{n}} \parallel L S [J] \rangle = -i\sqrt{2} \langle L' S' [J'] \parallel [S^{(1)} \otimes n^{(1)}]^{(1)} \parallel L S [J] \rangle \\ &= i\sqrt{6(2J+1)(2J'+1)} \left\{ \begin{array}{ccc} L' & L & 1 \\ S' & S & 1 \\ J' & J & 1 \end{array} \right\} \langle L' \parallel \hat{\mathbf{n}} \parallel L \rangle \langle S' \parallel \hat{\mathbf{S}} \parallel S \rangle. \end{aligned} \quad (\text{C.8})$$

Using the relation for the $9j$ symbol [34]

$$\begin{Bmatrix} L' & L & 1 \\ S & S & 1 \\ J' & J & 1 \end{Bmatrix} = \frac{(J' - L')(J' + L' + 1) - (J - L)(J + L + 1)}{\sqrt{24S(S+1)(2S+1)}} \cdot (-1)^{J+L'+S+1} \begin{Bmatrix} J' & J & 1 \\ L & L' & S \end{Bmatrix}, \quad (\text{C.9})$$

one eventually finds

$$\begin{aligned} & \langle L', S', [J'], T', K, K_3 | \hat{\mathbf{T}} \cdot (\hat{\mathbf{S}} \times \hat{\mathbf{n}}) | L, S, [J], T, K, K_3 \rangle \\ &= \frac{i}{2} (-1)^{2J+2L'+T+S+1+K} [(J' - L')(J' + L' + 1) - (J - L)(J + L + 1)] \\ & \quad \cdot \sqrt{T(T+1)(2T+1)(2J+1)(2J'+1)(2L+1)(2L'+1)} \\ & \quad \cdot \begin{Bmatrix} J' & J & 1 \\ L & L' & S \end{Bmatrix} \cdot \begin{Bmatrix} K & t & J' \\ 1 & J & T \end{Bmatrix} \cdot \begin{pmatrix} L' & 1 & L \\ 0 & 0 & 0 \end{pmatrix}. \end{aligned} \quad (\text{C.10})$$

Along the same lines one can express matrix elements of operators of (C.3) in the basis (C.2) through $6j$ symbols; the result is:

$$\begin{aligned} & \langle L', S', [J'], T', K, K_3 | \hat{\mathbf{S}} \cdot \hat{\mathbf{n}} | L, S, [J], T, K, K_3 \rangle \\ &= (-1)^{J+L'+S} \delta_{JJ'} \sqrt{(2L+1)(2L'+1)S(S+1)(2S+1)} \\ & \quad \cdot \begin{Bmatrix} J & S & L' \\ 1 & L & S \end{Bmatrix} \cdot \begin{pmatrix} L' & 1 & L \\ 0 & 0 & 0 \end{pmatrix}, \end{aligned} \quad (\text{C.11})$$

$$\begin{aligned} & \langle L', S', [J'], T', K, K_3 | \hat{\mathbf{T}} \cdot \hat{\mathbf{n}} | L, S, [J], T, K, K_3 \rangle \\ &= (-1)^{2J+2L'+S+T+K+1} \\ & \quad \cdot \sqrt{(2L+1)(2L'+1)(2J+1)(2J'+1)T(T+1)(2T+1)} \\ & \quad \cdot \delta_{SS'} \delta_{TT'} \begin{Bmatrix} K & T & J' \\ 1 & J & T \end{Bmatrix} \cdot \begin{Bmatrix} L' & J' & S \\ J & L & 1 \end{Bmatrix} \cdot \begin{pmatrix} L' & 1 & L \\ 0 & 0 & 0 \end{pmatrix}, \end{aligned} \quad (\text{C.12})$$

$$\begin{aligned} & \langle L', S', [J'], T', K, K_3 | \hat{\mathbf{S}} \cdot \hat{\mathbf{T}} | L, S, [J], T, K, K_3 \rangle \\ &= (-1)^{J+J'+L+S+T+K+1} \\ & \quad \cdot \sqrt{(2J+1)(2J'+1)(2S+1)S(S+1)T(T+1)(2T+1)} \\ & \quad \cdot \delta_{SS'} \delta_{TT'} \delta_{LL'} \begin{Bmatrix} K & T & J' \\ 1 & J & T \end{Bmatrix} \cdot \begin{Bmatrix} S & J' & L \\ J & S & 1 \end{Bmatrix}, \end{aligned} \quad (\text{C.13})$$

$$\begin{aligned}
& \langle L', S', [J'], T', K, K_3 | \hat{\mathbf{T}} \cdot (\hat{\mathbf{n}} \times \hat{\mathbf{L}}) | L, S, [J], T, K, K_3 \rangle \\
&= \frac{1}{2i} (-1)^{J+L'+L+T+S+K} [L'(L'+1) - L(L+1)] \\
&\quad \cdot \sqrt{T(T+1)(2T+1)(2J+1)(2J'+1)(2L+1)(2L'+1)} \\
&\quad \cdot \begin{Bmatrix} J' & J & 1 \\ L & L' & S \end{Bmatrix} \cdot \begin{Bmatrix} K & T & J' \\ 1 & J & T \end{Bmatrix} \cdot \begin{Bmatrix} L' & 1 & L \\ 0 & 0 & 0 \end{Bmatrix}. \quad (\text{C.14})
\end{aligned}$$

We checked these expressions using the commutation relations:

$$[\hat{\mathbf{S}} \cdot \hat{\mathbf{T}}, \hat{\mathbf{S}} \cdot \hat{\mathbf{n}}]_- = -i \hat{\mathbf{T}} \cdot (\hat{\mathbf{S}} \times \hat{\mathbf{n}}), \quad (\text{C.15})$$

$$[\hat{\mathbf{S}} \cdot \hat{\mathbf{T}}, \hat{\mathbf{T}} \cdot \hat{\mathbf{n}}]_- = i \hat{\mathbf{T}} \cdot (\hat{\mathbf{S}} \times \hat{\mathbf{n}}), \quad (\text{C.16})$$

$$[\hat{\mathbf{S}} \cdot \hat{\mathbf{n}}, \hat{\mathbf{T}} \cdot \hat{\mathbf{n}}]_- = 0. \quad (\text{C.17})$$

For practical calculations the $6j$ symbols and Clebsh-Gordan coefficients can be evaluated using e.g. *Mathematica*.

Appendix D

In this appendix we state the divergent parts of the sea energy (4.1) in the basis of the set of eigenfunctions of the free Dirac-Hamiltonian, given by eqs. (B.11–B.13). To this end a semiclassical expansion up to the quadratically divergent terms is performed. Subtraction of the result from the sea energy removes its quadratically divergent part for each value of the grand spin K separately. Since the quadratically divergent term is already complicated and lengthy in this basis, we do not continue the expansion to include also the logarithmic divergencies. Instead we use a simpler distribution of the total logarithmic divergence among the K sectors which may leave the separate sectors logarithmically divergent, but renders the sum over all K finite. Since the total value of the logarithmic divergence is small, the complete removal of all divergencies for each K is of little use and would cause an enormous increase of numerical effort.

We start from eq. (4.8) , insert eqs. (B.12, B.13), perform the sum \sum_r and obtain:

$$\begin{aligned}
E_{div} &= \sum_{K=0}^{\infty} (2K+1) \frac{1}{4\sqrt{\pi}} \int_0^1 \frac{dt}{t^{3/2}} \sum_{n=1}^{\infty} \frac{2e^{-tp_n^2}}{j_{K+1}^2(p_n R) R^3} \\
&\quad \cdot \int_0^R dx x^2 \sum_{i=1}^8 J_{K,i}(p_n x) \left[e^{-t(\mathcal{H}_K^2 - p_n^2)} \right]_{ii} J_{K,i}(p_n x) \Big|_{div}. \quad (\text{D.1})
\end{aligned}$$

We use the expansion

$$e^{-t(\mathcal{H}_K^2 - p_n^2)} = 1 - t(\mathcal{H}_K^2 - p_n^2) + \frac{t^2}{2}(\mathcal{H}_K^2 - p_n^2)^2 + \dots . \quad (\text{D.2})$$

The constant 1 is cancelled by subtraction of the vacuum (free field). Contributions to the quadratic divergence arise from the terms $\mathcal{O}(t)$, $\mathcal{O}(t^2 p_n^2)$ and $\mathcal{O}(t^2 K^2)$. The result is as follows:

$$E_{div,2} = \sum_{K=0}^{\infty} (2K+1) \frac{1}{2\sqrt{\pi}} \int_0^1 \frac{dt}{t^{1/2}} \sum_{n=1}^{\infty} \frac{e^{-tp_n^2}}{j_{K+1}^2(p_n R) R^3} \int_0^R dx x^2 F(x),$$

with

$$\begin{aligned} F(x) = & - \left\{ \delta_{K,0} \left[2m_F^2(j_1^2 + j_0^2)(H^2 + G^2 - 1) + (j_1^2 + j_0^2) \left(\tilde{A}^2 + \tilde{B}^2 + \frac{\tilde{C}^2}{4} \right) \right. \right. \\ & + (j_1^2 - j_0^2)(\tilde{A}' - \tilde{B}\tilde{C}) + (-3j_1^2 - j_0^2) \left(\frac{\tilde{A}}{x} \right) \left. \right] \\ & + (1 - \delta_{K,0}) \left[2m_F^2(j_{K+1}^2 + 2j_K^2 + j_{K-1}^2)(H^2 + G^2 - 1) \right. \\ & + \left(\frac{K+1}{2K+1} j_{K+1}^2 + j_K^2 + \frac{K}{2K+1} j_{K-1}^2 \right) (\tilde{A}^2 + \tilde{B}^2) + (j_{K+1}^2 + 2j_K^2 + j_{K-1}^2) \left(\frac{\tilde{C}^2}{4} \right) \\ & + \left(\frac{K+1}{2K+1} j_{K+1}^2 - j_K^2 + \frac{K}{2K+1} j_{K-1}^2 \right) (\tilde{A}' - \tilde{B}\tilde{C}) \\ & + \left. \left. \left(-\frac{(K+1)(2K+3)}{2K+1} j_{K+1}^2 - j_K^2 + \frac{K(2K-1)}{2K+1} j_{K-1}^2 \right) \left(\frac{\tilde{A}}{x} \right) \right] \right\} \\ & + \frac{t}{2} \left\{ \delta_{K,0} \left[(9j_1^2 + j_0^2) \left(\frac{\tilde{A}}{x} \right)^2 + (j_1^2 + j_0^2) \left(\frac{\tilde{B}}{x} \right)^2 \right. \right. \\ & + (j_1^2 + j_0^2) \tilde{C}^2 p_n^2 + \left(-\frac{9}{4} j_1^2 - \frac{1}{4} j_0^2 \right) \left(\frac{\tilde{C}}{x} \right)^2 \left. \right] \\ & + (1 - \delta_{K,0}) \left[\left(\frac{(K+1)(2K^2 + 7K + 9)}{2K+1} j_{K+1}^2 + (2K^2 + 2K + 1) j_K^2 \right. \right. \\ & + \left. \left. \frac{K(2K^2 - 3K + 4)}{2K+1} j_{K-1}^2 \right) \left(\frac{\tilde{A}}{x} \right)^2 \right. \\ & + \left. \left. \left((K+1)^2 j_{K+1}^2 + (2K^2 + 2K + 1) j_K^2 + K^2 j_{K-1}^2 \right) \left(\frac{\tilde{B}}{x} \right)^2 \right. \\ & + (j_{K+1}^2 + 2j_K^2 + j_{K-1}^2) \tilde{C}^2 p_n^2 \right. \end{aligned}$$

$$\begin{aligned}
& + \left(-\frac{8K^3 + 44K^2 + 50K + 9}{4(2K+1)} j_{K+1}^2 - \frac{4K^2 + 4K + 3}{2} j_K^2 \right. \\
& \left. - \frac{8K^3 - 20K^2 - 14K + 5}{4(2K+1)} j_{K-1}^2 \right) \left(\frac{\tilde{C}}{x} \right)^2 \Bigg\}, \tag{D.3}
\end{aligned}$$

where we have omitted the argument $(p_n x)$ of the Bessel-functions and denoted:

$$\tilde{A} \equiv \frac{1 - A(x)}{x}, \quad \tilde{B} \equiv \frac{B(x)}{x}, \quad \tilde{C} \equiv \frac{C(x)}{x}, \quad \tilde{A}' \equiv -\frac{1}{x} \frac{dA}{dx}(x). \tag{D.4}$$

To see whether this expression corresponds to the quadratically divergent part of eq. (4.3) we perform the limit $R \rightarrow \infty$ in which $j_{K+1}^2(p_n)R^3 \rightarrow R/p_n^2$ and $1/R \sum_n \rightarrow 1/\pi \int dp$. Using

$$\sum_K (2K+1) j_K^2(px) = 1, \quad \sum_K (2K+1)^3 j_K^2(px) = 1 + \frac{8}{3}(px)^2, \tag{D.5}$$

and performing the p integration we obtain:

$$\begin{aligned}
E_{div,2} = & -\frac{1}{\pi} \int_0^1 \frac{dt}{t^2} \int_0^\infty dx x^2 m_F^2 (H^2 + G^2 - 1) \\
& + \frac{1}{4\pi} \int_0^1 \frac{dt}{t} \int_0^\infty dx \left(\tilde{A}^2 + \tilde{B}^2 + \frac{5\tilde{C}^2}{4} \right). \tag{D.6}
\end{aligned}$$

The first term coincides with the quadratically divergent part of eq. (4.3), as it should do. The second term is logarithmically divergent so that the remaining logarithmic divergence of eq. (4.3) to be removed is therefore:

$$\begin{aligned}
E_{div,1} = & \frac{1}{2\pi} \int_0^1 \frac{dt}{t} \int_0^\infty dx g(x), \\
g(x) = & \frac{1}{6} \left[\left(A' + \frac{BC}{x} \right)^2 + \left(B' - \frac{AC}{x} \right)^2 + \frac{(A^2 + B^2 - 1)^2}{2x^2} \right] \\
& + m_F^4 x^2 \left[(G^2 + H^2)^2 - 1 \right] \\
& + \frac{m_F^2}{2} \left[(G^2 + H^2)(1 + A^2 + B^2 + C^2/2) + 2A(G^2 - H^2) - 4BGH \right. \\
& \left. + 2x^2(G'^2 + H'^2) - 2xC(HG' - H'G) \right] - \frac{(1 - A)^2 + B^2 + \frac{5C^2}{4}}{2x^2}. \tag{D.7}
\end{aligned}$$

This divergence can be distributed among the K sectors as follows:

$$E_{div,1} = \sum_{K=0}^{\infty} (2K+1) \frac{1}{2\sqrt{\pi}} \int_0^1 dt t^{1/2} \sum_{n=1}^{\infty} \frac{e^{-tp_n^2}}{j_{K+1}^2(p_n R) R^3} \int_0^R dx x^2 G(x)$$

with

$$G(x) = \left[\delta_{K,0} \left(j_1^2(p_n x) + j_0^2(p_n x) \right) + (1 - \delta_{K,0}) \left(j_{K+1}^2(p_n x) + 2j_K^2(p_n x) + j_{K-1}^2(p_n x) \right) \right] \frac{g(x)}{x^2}. \quad (\text{D.8})$$

As already mentioned, we would obtain a much more complicated distribution of the logarithmic divergence among the K sectors if we continued the expansion eq. (D.2) up to fourth order and collected the logarithmically divergent terms. Although the simpler version eq. (D.8) removes the logarithmic divergencies only after summing over K and not for each K separately, it is sufficient for all numerical purposes to use this formula.

Let us finally remark that one can in principle use a simpler formula also for the quadratically divergent terms which can be obtained by expanding eq. (D.2) in a large K limit. This leads to an expression for $E_{div,2}$ similar to eq. (D.3) but contains only the first term $H^2 + G^2 - 1$. Numerically identical results are obtained with this version, but one needs higher numerical parameters to insure stability, so that the numerical effort is increased.

References

- [1] L.D.Faddeev, "Looking for multi-dimensional solitons", in: Non-local Field Theories, Dubna (1976)
- [2] R.Jackiw and C.Rebbi, *Phys. Rev. Lett.* **37** (1976) 172
- [3] G.'t Hooft, *Phys. Rev. Lett.* **37** (1976) 8
- [4] V.Rubakov and A.Tavkhelidze, *Phys. Lett.* **B165** (1985) 109;
V.Rubakov, *Prog. Theor. Phys.* **75** (1986) 366;
V.Matveev, V.Rubakov, A.Tavkhelidze and V.Tokarev, *Nucl. Phys.* **B282** (1987) 700
- [5] D.Diakonov and V.Petrov, *Phys. Lett.* **275B** (1992) 459
- [6] P.Arnold and L.McLerran, *Phys. Rev.* **D36** (1987); *ibid.* **37** (1988) 1020
- [7] D.Diakonov and M.Polyakov, *Nucl. Phys.* **B389** (1993) 109
- [8] D.Diakonov and V.Petrov, *Preprint* Ruhr-Universität Bochum, TPII-52/93
- [9] V.Kuzmin, V.Rubakov and M.Shaposhnikov, *Phys. Lett.* **B191** (1987) 171
- [10] M.Shaposhnikov, *Nucl. Phys.* **B287** (1987) 757; **B299** (1988) 797

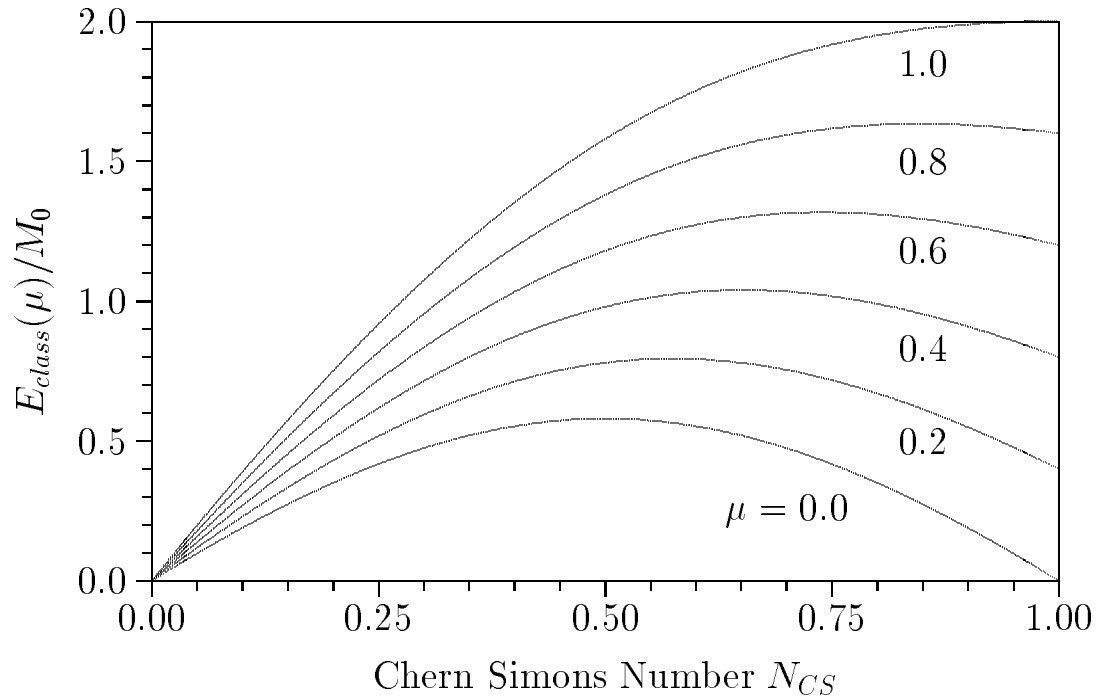
- [11] R.Dashen, B.Hasslacher and A.Neveu, *Phys. Rev.* **D10** (1974) 4138
- [12] N.Manton, *Phys. Rev.*, **D28** (1983) 2019;
F.R.Klinkhamer and N.S.Manton, *Phys. Rev.* **D30** (1984) 2212
- [13] T.Akiba, H.Kikuchi and T.Yanagida, *Phys. Rev.* **D38** (1988) 1937
- [14] J.Kunz and Y.Brihaye, *Phys. Lett.* **B216** (1989) 353;
Y.Brihaye and J.Kunz, *Mod. Phys. Lett.* **A4** (1989) 2723
- [15] J.Kunz, B.Kleihaus and Y.Brihaye, *Phys. Rev.* **D46** (1992) 3587
- [16] J.Kunz and Y.Brihaye, *Phys. Lett.* **B304** (1993) 141;
Phys. Rev. **D48** (1993) 5905
- [17] E.Witten, *Phys. Lett.* **117B** (1982) 432
- [18] D.Diakonov, V.Petrov and A.Yung, *Sov. J. Nucl. Phys.* **39** (1984) 150;
D.Diakonov, V.Petrov and A.Yung, *Phys. Lett.* **130B** (1984) 240
- [19] A.Bochkarev and M.Shaposhnikov, *Mod. Phys. Lett.* **A2** (1987) 417
- [20] L.Carson and L.McLerran, *Phys. Rev.* **D41** (1990) 647
- [21] L.Carson, X.Li, L.McLerran and R.-T.Wang, *Phys. Rev.* **D42** (1990) 2127
- [22] J.Baacke and S.Junker, *Preprint* Dortmund University, DO-TH-93/19
- [23] A.Bochkarev, *Phys. Lett.* **B254** (1991) 165
- [24] T.Gould and I.Rothstein, *Preprint* Johns Hopkins University Baltimore,
JHU-TIPAC-930001, University of Michigan, UM-93-02
- [25] J.Langer, *Ann. Phys. (N.Y.)* **41** (1967) 108; *ibid.* **54** (1969) 258
- [26] I.Affleck, *Phys. Rev. Lett.* **46** (1981) 388
- [27] S.Khlebnikov and M.Shaposhnikov, *Nucl. Phys.* **B308** (1988) 885
- [28] D.Gross, R.Pisarski and L.Jaffe, *Rev. Mod. Phys.* **53** (1981) 43
- [29] T.Akiba, H.Kikuchi and T.Yanagida, *Phys. Rev.* **D40** (1989) 588
- [30] D.A.Kirzhnitz and A.D.Linde, *Ann. Phys.* **101** (1976) 195
- [31] D.Diakonov, V.Petrov and P.Pobylitsa, *Nucl. Phys.* **B306** (1988) 809
- [32] S.Kahana and G.Ripka, *Nucl. Phys.* **A429** (1984) 962;
G.Ripka and S.Kahana, *Phys. Rev.* **D36** (1987) 1233
- [33] Th.Meissner, F.Grümmer and K.Goeke, *Phys. Lett.* **B306** (1989) 296;
Th.Meissner, E.Ruiz Arriola and K.Goeke, *Z. Phys.* **A336** (1990) 91;
K.Goeke et al., *Phys. Lett.* **B256** (1991) 321

[34] D.A.Varshalovich, A.N.Moskalev and V.K.Khersonskii, *"Quantum theory of angular momentum"*, World Scientific, 1988

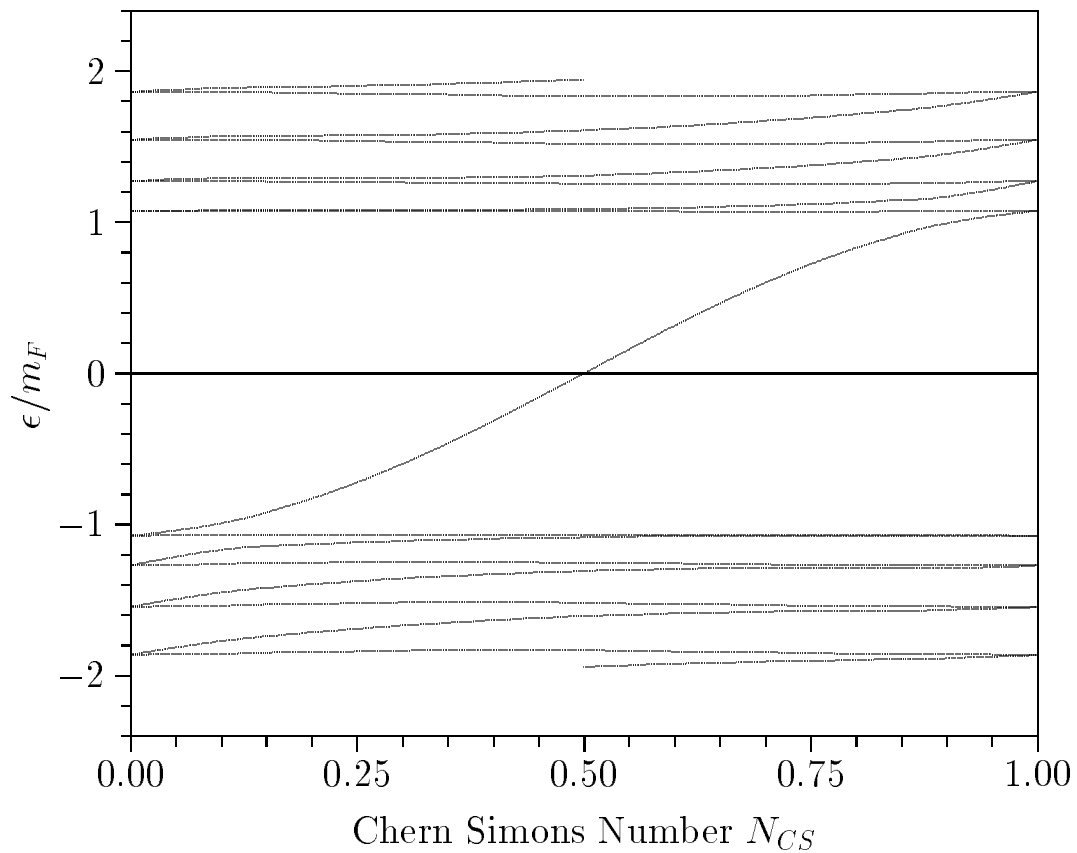
Figure captions

1. Energy barrier as a function of N_{CS} for different values of the chemical potential μ for $m_H = m_W$. The units for $E_{class}(\mu)$ and μ are $M_0 = \mu_{crit} = 2\pi m_W/\alpha$.
2. The discrete level ε_{val} and some discretized continuum eigenstates as a function of N_{CS} for $m_F = m_W$. It is demonstrated that each level is shifted upwards and finally takes the position of its predecessor.
3. The renormalized fermionic energy E_{fer}^{ren} as a function of N_{CS} for the fermion masses $m_F/m_W = 0, 1$ and 2 . It has to be compared with the classical energy which is about $100 m_W$ for $N_{CS} = 0.5$.
4. The fermionic temperature dependent part βE_{fer}^{temp} (solid lines) and the classical part βE_{class}^{ren} (dashed lines) of the sphaleron transition rate as a function of T for $m_t/m_W = 1.5, 2.0$ and 2.5 . E_{class}^{ren} and E_{fer}^{temp} are defined in eqs. (5.20, 5.21).
5. The baryon density as a function of the radial distance r for $m_F = m_W$ and $N_{CS} = 0.26, 0.5, 0.74$, and close to 1 .

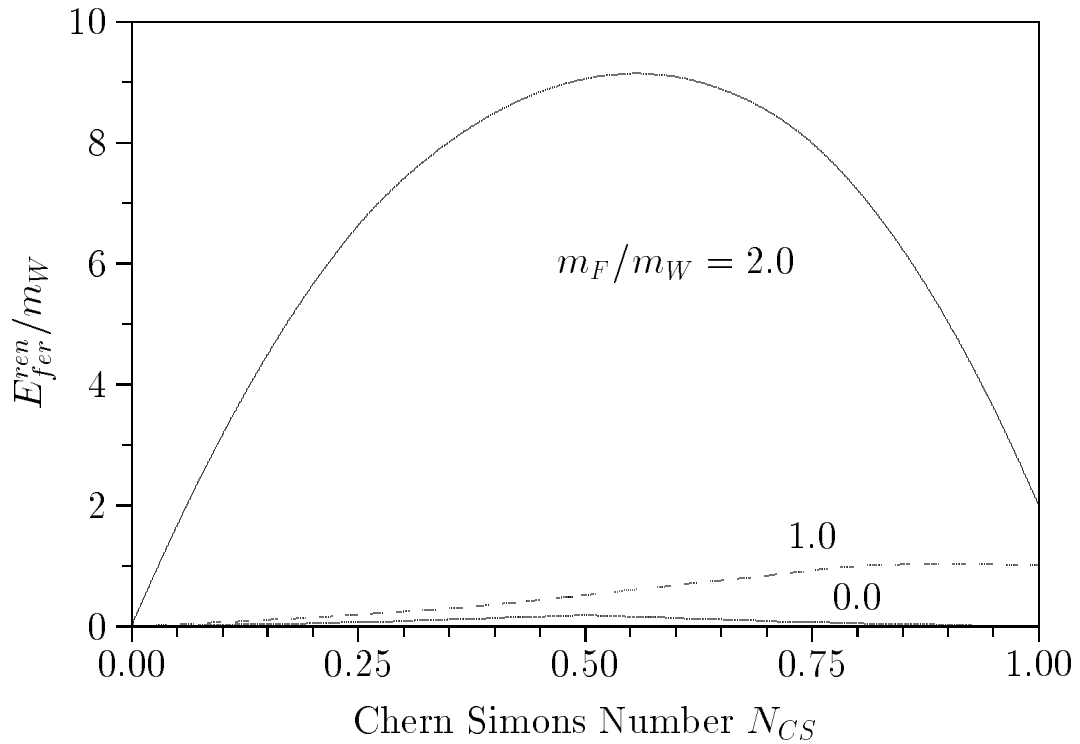
Minimal Energy Paths for Different μ



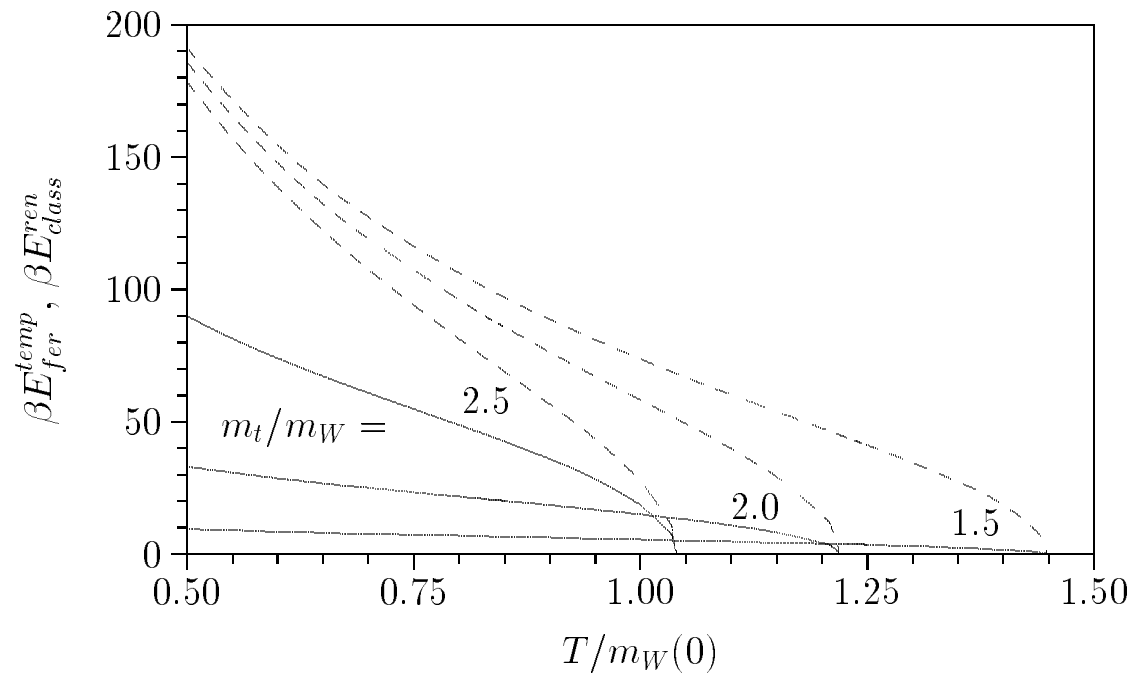
$K = 0$ Eigenstates during Transition



Renormalized Fermionic Energy



Transition Rate



Baryon Densities for Different N_{CS}

